AALBORG UNIVERSITY

DENMARK

Hydrothermal liquefaction of wood using a modified multistage shrinking-core model

Jayathilake, Madhawa; Rudra, Souman; Rosendahl, Lasse

Link to publication from Aalborg University

Full Length Article

Hydrothermal liquefaction of wood using a modified multistage shrinking-core model

Madhawa Jayathilake[a], Souman Rudra[a,*], Lasse A. Rosendahl[b]
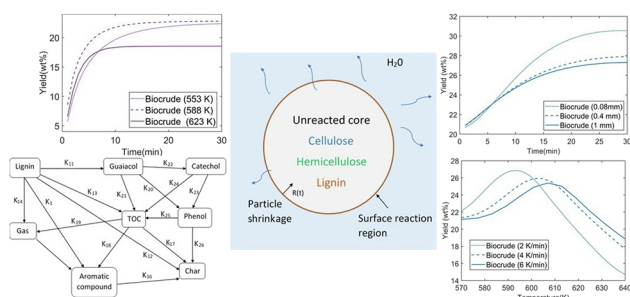
[a] Department of Engineering Sciences, University of Agder, Jon Lilletuns vei 9, 4879 Grimstad, Norway
[b] Department of Energy Technology, Aalborg University, Pontoppidanstræde 101, 9220 Aalborg, Denmark

GRAPHICAL ABSTRACT

ARTICLE INFO

ABSTRACT

Wood liquefaction in hot compressed water is modeled using the hydrolysis of Cellulose, Hemicellulose, and Lignin. These three components are reacted under catalyst-free subcritical conditions in a temperature range from 553 K to 640 K, and the heating rate ranges from 2 K/min to 6 K/min. Using a simplified reaction scheme, water-soluble products[1] (WSP), Biocrude, char, and gas are generated through intermediates with each wood component. A modified multistage shrinking core model is employed to simulate biomass particle degradation. The reaction and kinetic regime of the hydrothermal liquefaction[2] (HTL) process are treated separately for each wood component. Although the lack of initial fast reaction kinetic data limits the development of more accurate models, computed results displayed a generous fit to data from the literature. At 593 K for a 2 K/min heating rate and particle size of 0.08 mm, biocrude shows the maximum yield of 26.87% for wood liquefaction. Although lower heating rates show fast initial lignin hydrolysis, for longer residence times, and close to the critical point, yield outputs show similar yields. Meanwhile, char and gas yields of cellulose model show maximums of 55 wt% and 25 wt% respectively at 640 K with a 2 K/min heating rate. Nevertheless, char yield values become very similar at 640 K for different heating rates for the cellulose hydrolysis model. Both cellulose and lignin hydrolysis models show better hydrolysis with smaller particle sizes. Besides, lignin decomposition shows more dependence on the particle size, where it decomposes much faster with 0.08 mm particle and slower than Cellulose with the 1 mm particle.

1. Introduction

Hydrothermal liquefaction (HTL) is a thermochemical conversion method which mainly produces a liquid crude oil. In the HTL process, initially, the biomass is decomposed into smaller molecules through hydrolysis [1]. HTL process and hydrolysis of wood in subcritical and supercritical water have been widely investigated recently [2–7]. Besides, the main components of wood are also used to study the hydrolysis such as cellulose and Lignin [8–18]. Radical decomposition of Cellulose to oligosaccharides and monosaccharides at 513 K is investigated where the latter showcased heating rates below 1 K/s affected the cellulose hydrolysis [10,11]. As the most abundant component of woody biomass, Cellulose is widely used for hydrolysis studies. The increase of hydrolysis products in supercritical water and the kinetics of cellulose hydrolysis in the sub and supercritical water is also proposed successfully with a grain model by Sasaki et al. [14,15,17]. Cellulose and glucose decomposition pathways in hot compressed water under catalysts free conditions are investigated by Minowa et al. [19]. A study by Kabyemela et al. [20] observed the forward epimerization of glucose to fructose in subcritical temperatures, where backward epimerization from fructose to glucose is found to be negligible. Glucose is decomposed quickly from 573 K to 623 K [20]. Although the activation energies for glucose decomposition to fructose did not differ much around critical point, 5-hydroxyl-methyl-furfural (5-HMF) reaction kinetics are drastically changed around 603 K due to ionic product and low density of water [21].

Yong and Matsumara [9] extensively studied the lignin decomposition in the subcritical conditions and came up with a comprehensive reaction scheme. According to Yong and Matsumara [9], most of the reaction rate constants of lignin decomposition followed the Arrhenius behavior where some of the reactions follow a non-Arrhenius behavior. Zhang et al. [22] proposed a kinetic model with kinetic data for Kraft lignin decomposition and suggested the kraft pine lignin followed a two-phase decomposition scheme. Forchheim et al. [23] successfully estimated the phenolic products from lignin hydrothermal depolymerization with another kinetic model where they discussed some tendencies of gas and solid residue behavior in variable operating conditions.

Hydrolysis studies on hemicellulose are not abundantly found. Pronyk and Mazza [13] proposed a monophasic and biphasic reaction mechanism for hemicellulose hydrolysis. The contribution from hemicellulose to biocrude is quite small as the production of furfural from hemicellulose is found to be considered insignificant after 443 K [13]. A recent review by Delbecq et al. [24] extensively discussed the furfural synthesis from bio-based products where the hydrolysis of hemicellulose and derivatives are analyzed and optimized. Hemicellulose (Xylan) produced its maximum hydrolysis yield at a low-temperature value of 493 K-508 K [25] or even lower temperatures such as 473 K [26]. With higher temperatures, the hydrolysis of xylan is decreased significantly, and ultimately xylose, and then furfural production is decreased [26].

Various approaches are used to model the hydrolysis of wood and the decomposing method of the wood, while the shrinking core approach is one of the main criteria used [7,10,11,27]. Galegano and Blasi [27] and Kamio et al. [10,11] used the unreacted shrinking core concept to model pyrolysis and hydrolysis, respectively, by using the same particle decomposition concept in two different thermochemical processes. Mosteiro-Romero et al. [7] developed a mathematical model on wood hydrolysis with a shrinking core model, which was developed upon well designed experimental data. It was able to predict the hydrolysis products yields to a convincing extent, which were modeled as lump components.

1.1. Shrinking core approach and hydrolysis modeling

Hydrolysis modeling of wood with kinetic models is scarce [7].

Frequently, model compounds are abundantly used for the kinetic models of hydrolysis studies [4,5,8–11,13,22,25]. Besides, the proposed model is influenced by the model developed by Kamio et al. [11] for cellulose hydrolysis.

Kamio et al. [11] developed a single particle system in subcritical conditions for cellulose hydrolysis with a shrinking core approach for the particle, where reduction of the particle occurs only in the radial direction. Due to a surface reaction on the particle surface, cellulose particle is hydrolyzed by the water monomer and result in producing oligosaccharides to the system. Then the oligosaccharides are further hydrolyzed into monosaccharides where it is then hydrolyzed into degradation products. Here the oligosaccharides represent the glucose units, and monosaccharides represent glucose and fructose. Degradation products represent the decomposition products from monosaccharides as overall.

In the proposed model, wood hydrolysis is modeled using the hydrolysis of three main components of wood. Each wood component has its hydrolysis reaction mechanism and will produce hydrolysis products. It is proposed to model the wood hydrolysis by using the cumulative effect of each hydrolysis model from the three wood components. The decomposition of the wood particle is assumed to be only in the radial direction. Thus, the modeling criteria used in this model are a shrinking core model. Fig. 1 below shows a graphical model of the assumed shrinking core concept used for the proposed model.

The modeling criteria of the shrinking core model is based on the model proposed by Kamio et al. [11], Galegano and Blasi [27], and Mosteiro-Romeiro et al. [7]. Reactions used in this model are divided into cellulose reactions, lignin reactions, and hemicellulose reactions.

Despite the various studies on hydrolysis studies on each component of wood separately, there is a lack of models of studying the behavior and role of each wood component in the overall wood liquefaction. By developing a model with having all the three main components of wood, the effect of each component hydrolysis on wood hydrolysis can be studied. Moreover, the contribution of each component on the liquefaction outputs can be thoroughly investigated. Therefore, a mathematical model for decomposition of wood in subcritical temperature is developed using a modified shrinking core model where a custom reaction kinetic rate is developed to hydrolysis of each wood component. Wood consists of Cellulose, Lignin, and hemicellulose. Although the hydrolysis of each component is treated separately, core shrinkage is modeled as a cumulative effect of hydrolysis of each component. Hence, this model simulates wood decomposition by using three main components of wood. Furthermore, the behavior of each component and their distribution in different outputs can be studied with this model. The hydrolysis of each component is used as the initial reaction of the process. The diffusion of water monomers to the particle surface to initiate hydrolysis and dissolution of the products in water is also given importance during the modeling process. Once the degradation process
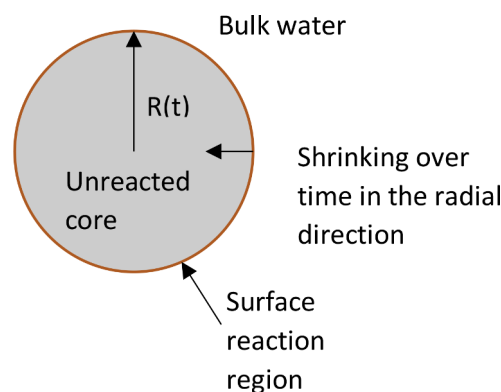

Fig. 1. Shrinking core model assumed for the hydrolysis of the wood particle of model components submerged in water.

is underway with heterogeneous hydrolysis, the dissolved compounds will further hydrolyze with homogeneous hydrolysis and behave according to the kinetic model. More chemical compounds are incorporated in the model, and chemical reactions of those chemical compounds are used rather than using lump components. In the developed model, the kinetic reaction rate constants vary according to the temperature. Since the temperature is changed during the process, the Arrhenius equation [28] is used to calculate the fluctuating rate constants. Additionally, kinetic parameters from the literature are used for the initial kinetic data for the mathematical model.

2. Method

2.1. Decomposition of the biomass particle

In the proposed model, initially, the particle is considered as a combination of Cellulose, hemicellulose, and Lignin. At different temperatures, according to the reaction kinetics, each component is started hydrolyzing. The hydrolysis of each component is determined by the developed reaction rate constant (Shown later in the modeling process). The overall biomass particle decomposition is assumed to be a cumulative effect of each component and in the radial direction. As Kamio et al. [11] proposed, diffusion of the water monomer through the aqueous film surrounding the biomass particle is modeled using the mass transfer of water.

$$M_w = 4\pi r^2 k_A (C_B - C_S) \tag{1}$$

M_w represent the mass transfer rate of the water monomer, r is the radial position of the particle, k_A is the mass transfer coefficient, C_B represents the bulk water monomer concentration, and C_S is the water concentration at the surface.

Hydrolysis of the biomass particle is expressed below, where M_B is the hydrolysis reaction rate at the surface of each wood component k_H is the hydrolysis rate constant.

$$M_B = 4\pi r^2 k_H C_S \tag{2}$$

Assuming the overall rate constant of hydrolysis of the biomass particle k_H is the sum of hydrolysis rate constants of three wood components. Below, equation (3) shows the overall hydrolysis rate constant of the biomass particle hydrolysis.

$$k_H = k_1 + k_5 + k_{10} + k_{11} + k_{12} + k_{13} + k_{14} + k_{26} \tag{3}$$

(k_H becomes a different value according to the wood component, which is being hydrolyzed. As an example, if only Cellulose is being hydrolyzed $k_H = k_1 + k_5$ while, if both Cellulose and hemicellulose are being hydrolyzed $k_H = k_1 + k_5 + k_{26}$. Therefore, at different time intervals, the particle decomposes at different rates.)

At steady-state condition, as mass transfer should be equal between water and biomass particle, from (1) and (2)

$$r_w = \frac{4\pi r^2 C_B}{\frac{1}{k_A} + \frac{1}{k_H}} \tag{4}$$

r_w represents the reaction rate of the water monomer for one biomass particle. When the decomposition rate is described in a point of view in the mass balance of a biomass particle and when the radius of the particle is r,

$$\frac{d(4\pi r^3 \rho / 3)}{dx} = -r_B \tag{5}$$

Here r_B is the reaction rate of the biomass molecule for a unit biomass particle, and ρ is the molar density of the biomass particle. (ρ changes according to each wood component) Therefore, with stoichiometry,

$$-r_w = \beta r_B \tag{6}$$

where β represents the stoichiometry value of water in the hydrolysis reaction.

(In the proposed model, it is assumed that the biomass particle is consist of 45% of Cellulose, 25% Hemicellulose, and 30% of Lignin)

Substituting (4) and (6) to (5),

$$4\pi r^2 \rho \frac{dr}{dt} = \frac{4\pi r^2 C_B}{\frac{1}{k_A} + \frac{1}{k_H}} \tag{7}$$

When the radial position of the surface becomes r, the decomposition ratio of the biomass particle can be written as,

$$1 - x = \frac{\frac{4}{3}\pi r^3 \rho}{\frac{4}{3}\pi r_0^3 \rho} = \left(\frac{r}{r_0}\right)^3 \tag{8}$$

where, x is the decomposition ratio of a unit biomass particle. After derivation over time,

$$-\frac{dx}{dt} = \frac{3r^2}{r_0^3} \frac{dr}{dt} \tag{9}$$

By substituting from (8) and (9) to (7),

$$\frac{4\pi r_0^3}{3} \rho \frac{dx}{dt} = \frac{4\pi r_0^2 C_B (1-x)^{\frac{2}{3}}}{\beta \left(\frac{1}{k_A} + \frac{1}{k_H}\right)} \tag{10}$$

When the decomposition of the biomass particle is expressed by the concentration of each wood component molecules, x can be expressed, as shown below in equation (11).

$$x = \frac{\sum (C_{modi,0} - C_{modi})}{\sum C_{modi,0}} \tag{11}$$

where $C_{modi,0}$ is the concentration of each wood component molecule at t = 0, and C_{modi} is the concentration of each wood component molecule at t = t.

From (11),

$$r_B = \frac{dx}{dt} = \frac{3C_B (1-x)^{\frac{2}{3}}}{r_0 \beta \rho \left(\frac{1}{k_A} + \frac{1}{k_H}\right)} \tag{12}$$

Therefore substituting (11) into (12),

$$r_d = \frac{dC_{bio}}{dt} = -k_x \sum C_{modi}^{\frac{2}{3}} \tag{13}$$

where $i = 1, 2, 3$

Here, r_d is the decomposition rate of the biomass particle, k_x is the rate coefficient of biomass decomposition and C_{modi} is the concentration of each wood component. Therefore,

$$k_x = \frac{3C_B \sum C_{modi,0}^{\frac{1}{3}}}{r_0 \beta \rho \left(\frac{1}{k_A} + \frac{1}{k_H}\right)} \tag{14}$$

According to the wood component or components, which are being hydrolyzed, k_x becomes a different rate constant due to the change in k_H.

All the rate constants are changed with temperature. Since the temperature is changed during the process Arrhenius equation can be used to calculate the changing rate constants.

$$k_{i,t} = k_{0,i} e^{\frac{-E_a}{RT}} \tag{15}$$

where, $k_{i,t}$ is the calculated rate constant, $k_{o,i}$ is the frequency factor and, E_a is the Activation energy for each component. Arrhenius law can be applied to all the reactions in the process since the rate constants are changed with temperature. Moreover, the heating process can be expressed by the following equation 16.

Heating process; $T = \vartheta_T t + T_{ini}$ \hfill (16)

where, ϑ_T is the heating rate, t represents time and, T_{ini} is the initial temperature.

By substituting to (13) from (14), (15), and (16), an equation for

biomass decomposition can be developed.

Differential equations developed to calculate the change in yield of each component in the system is listed in the appendix.

The model predicted values are compared and validated with the experimental values in literature. Theoretical values of each chemical component are calculated from differential equations A1-A18 using the backward Euler method. According to the required initial concentration of each component of wood in the system (given that different wood types have different ratios of each wood component) number of moles of each wood, component is calculated and inserted. From the differential equations, the variation of the concentrations of each chemical compound is obtained. Then for each wood component, each chemical compound or resultant phase is presented as a percentage of the input. For the calculations in the developed model, it is assumed no losses during the extraction process, as well as the carbon recovery is > 99%.

2.2. Cellulose hydrolysis model

The reaction mechanisms for Cellulose are influenced by the reaction mechanism proposed by Cantero et al. [21] Minowa et al. [19] and Kamio et al. [11]. According to Kamio et al. [11], Cantero et al. [21], Sasaki et al. [14,15,17] and Minowa et al. [19] from the hydrolysis of Cellulose, water-soluble intermediates are formed. Then the further hydrolysis, polymerization, dehydration, and decomposition creates the degradation products from the intermediates such as water-soluble products (aqueous phase), biocrude, gas, and char. As the secondary char is hard to quantify experimentally, both primary and secondary char produced is taken as a lump component. Fig. 2 shows the reaction pathway used for the cellulose hydrolysis and decomposition during the liquefaction process. Table 1 shows the type of each reaction used in the cellulose hydrolysis model.

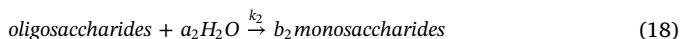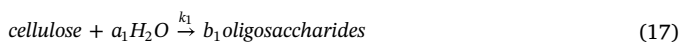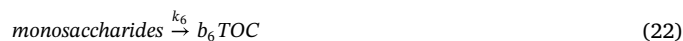Below equations from 17 to 25 show the reactions incorporated in the cellulose liquefaction model.
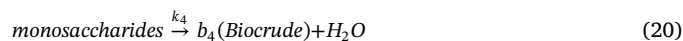
$$cellulose + a_1H_2O \xrightarrow{k_1} b_1 oligosaccharides \qquad (17)$$

$$oligosaccharides + a_2H_2O \xrightarrow{k_2} b_2 monosaccharides \qquad (18)$$
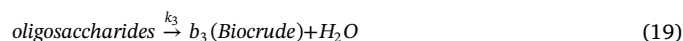
Table 1
Reaction type of each reaction used in the cellulose liquefaction model.

Kinetic parameter	Reaction type	Kinetic parameter	Reaction type
K_1	Hydrolysis	K_6	Decomposition
K_2	Hydrolysis	K_7	Decomposition
K_3	Dehydration	K_8	Polymerization
K_4	Dehydration	K_9	Decomposition
K_5	Dehydration	K_{10}	Polymerization

$$oligosaccharides \xrightarrow{k_3} b_3 (Biocrude) + H_2O \qquad (19)$$

$$monosaccharides \xrightarrow{k_4} b_4 (Biocrude) + H_2O \qquad (20)$$

$$cellulose \xrightarrow{k_5} b_5 Char + H_2O \qquad (21)$$

$$monosaccharides \xrightarrow{k_6} b_6 TOC \qquad (22)$$

$$Biocrude \xrightarrow{k_7} b_7 TOC \qquad (23)$$

$$TOC \xrightarrow{k_8} b_8 Char + b_9 CO_2 \qquad (24)$$

$$Biocrude \xrightarrow{k_{10}} b_{10} Char \qquad (25)$$

a_i is the stoichiometry value for water for each hydrolysis reaction. (where $i = 1,2$)
b_i is the stoichiometry value for the reaction output for each reaction. (where $i = 1,2, 3…,10$)

Micro-crystalline Cellulose, which is consisted of 230 glucose molecules, is used to model the cellulose component. Although oligosaccharides are supposed as a mix of cellobiose, cellotriose, and cellotetraose, for simplification, the kinetic data related to cellobiose is chosen for the model. Furthermore, monosaccharides are a mix of glucose and fructose, where the kinetic data for glucose decomposition is used for the model. 'Biocrude" is supposed to be a mix of chemicals such as glycolaldehyde, glyceraldehyde, erythrose, pyruvaldehyde, dihydroxyacetone, furfural, and 5-hydroxymethyl-2-furaldehyde (5-HMF)
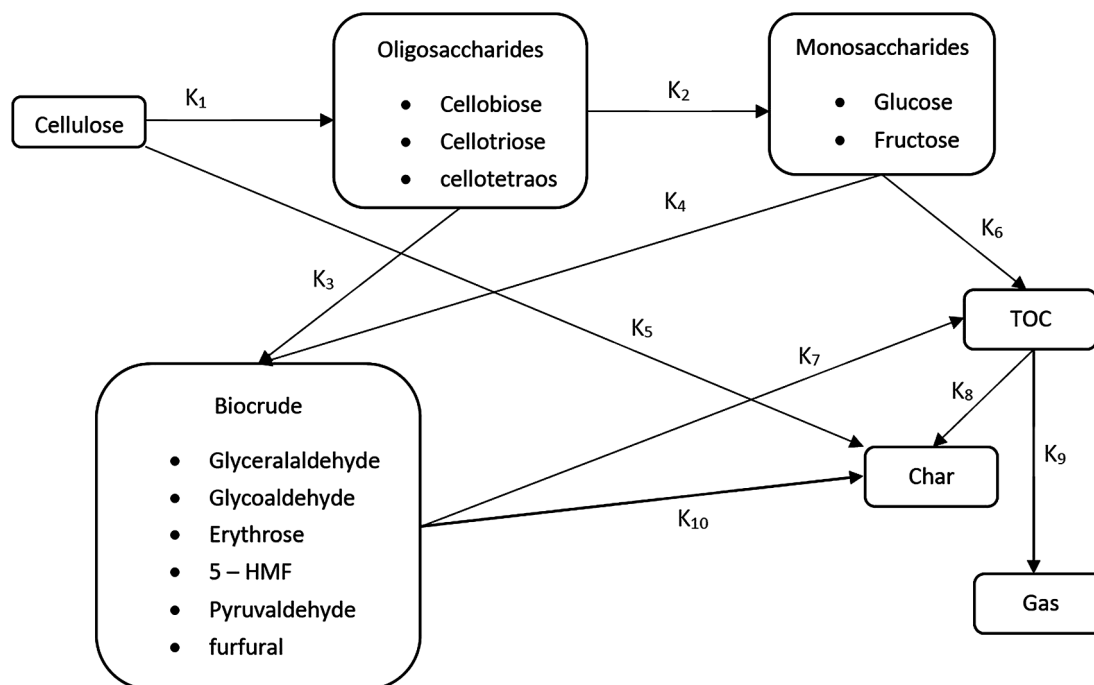

Fig. 2. Reaction pathway of cellulose decomposition.

[29]. Therefore 'Biocrude' represents the biocrude phase produced by the cellulose liquefaction. For the calculations, kinetic data for 5-HMF is used in the model for '*Biocrude.*' For the cellulose hydrolysis model, required kinetic parameters are taken from the literature [11,14,15,17,19–21,29,30]. Due to the simplified reaction scheme for cellulose hydrolysis and decomposition, some of the important conversions, such as the formation of phenolic compounds from Cellulose [18,31], are not included as separate chemical reactions.

The term 'TOC' is used to indicate the water-soluble organics in the aqueous phase from cellulose hydrolysis except for Cellulose, light aldehydes (except 5-HMF, glycolaldehyde, glyceraldehyde.) and carboxylic acids. In the cellulose hydrolysis model, Cellulose is considered as the biomass. Biocrude is assumed to consist of glycolaldehyde, glyceraldehyde, erythrose, pyruvaldehyde, dihydroxyacetone, furfural, and 5-hydroxymethyl-2-furaldehyde (5-HMF). TOC is assumed to consist of water-soluble organics. Even though light aldehydes and carboxylic acids can be dissolved in water, those compounds are considered as a part of the biocrude phase.

2.3. Lignin hydrolysis model

The lignin hydrolysis mechanism is based on the kinetic study and reaction pathways proposed by Yong and Matsumara [9] and Fang et al. [32], where the kinetic data is based on Yong and Matsumara [9], Zhang et al. [22], Forchheim et al. [23], and Arturi et al. [33]. Yong and Matsumara proposed a detailed reaction scheme for lignin hydrolysis, which consists of a gas phase, char, an aqueous phase, and another phase consist of phenols, TOC, Aromatics, Guaiacol. With further secondary hydrolysis reactions, some of the hydrolysis products decompose into tertiary components, which are also included in this model. In the proposed model, the shrinking core concept relates to the primary or the heterogenous hydrolysis reactions. Secondary decomposition, polymerization, and dehydration reactions are modeled using a conventional kinetic model, which is not being observed with other models that have used the shrinking core concept. Below, Fig. 3 shows the used reaction pathway of hydrolysis and decomposition of Lignin during the liquefaction process.

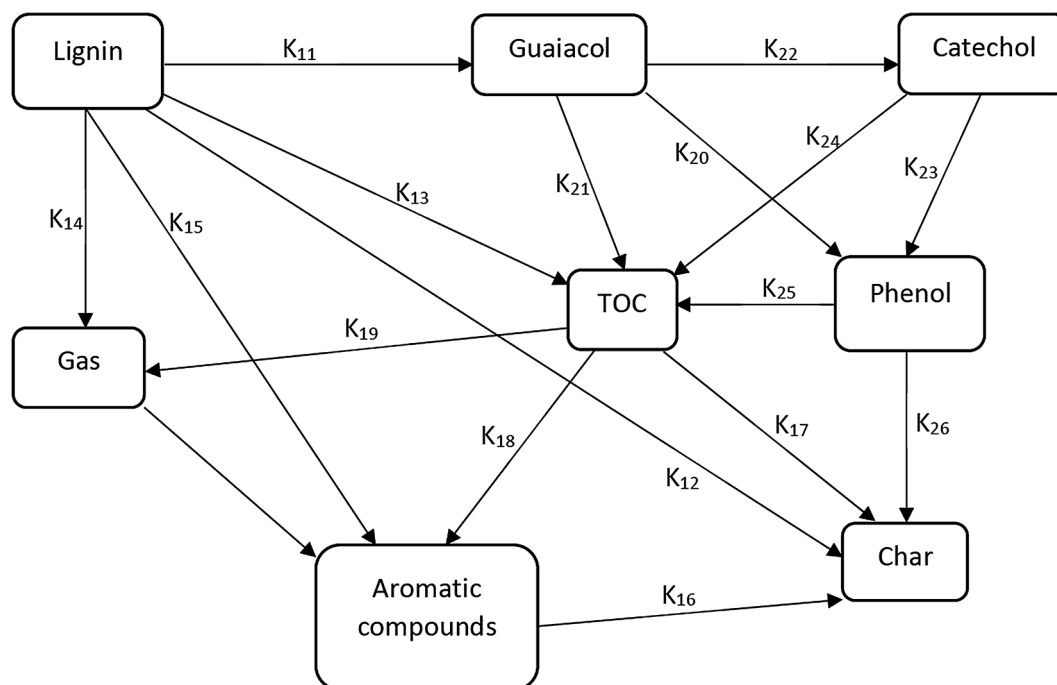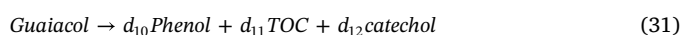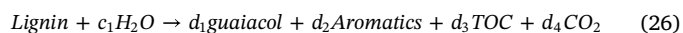For the lignin liquefaction model, required kinetic parameters are

Table 2
Reaction type of each reaction used in the lignin liquefaction model.

Kinetic parameter	Reaction type	Kinetic parameter	Reaction type
K_{11}	Hydrolysis	K_{19}	Gasification
K_{12}	Dehydration	K_{20}	Decomposition
K_{13}	Hydrolysis	K_{21}	Decomposition
K_{14}	Hydrolysis	K_{22}	Decomposition
K_{15}	Hydrolysis	K_{23}	Decomposition
K_{16}	Polymerization	K_{24}	Decomposition
K_{17}	Polymerization	K_{25}	Decomposition
K_{18}	Decomposition	K_{26}	Polymerization

taken from the literature [9,22,23,34,35]. Table 2 shows the type of each reaction used in the lignin hydrolysis model.

Below equations from 26 to 34 show the reactions incorporated in the lignin liquefaction model.

$$Lignin + c_1 H_2 O \rightarrow d_1 guaiacol + d_2 Aromatics + d_3 TOC + d_4 CO_2 \quad (26)$$

$$Lignin \rightarrow d_5 char + H_2 O \quad (27)$$

$$Aromatics \rightarrow d_6 char \quad (28)$$

$$TOC \rightarrow d_7 char \quad (29)$$

$$TOC \rightarrow d_8 Aromatics + d_9 CO_2 \quad (30)$$

$$Guaiacol \rightarrow d_{10} Phenol + d_{11} TOC + d_{12} catechol \quad (31)$$

$$Catechol \rightarrow d_{13} Phenol + d_{14} TOC \quad (32)$$

$$Phenol \rightarrow d_{15} TOC \quad (33)$$

$$Phenol \rightarrow d_{16} Char \quad (34)$$

c_i is the stoichiometry value for water for each hydrolysis reaction. (where $i = 1$)
d_i is the stoichiometry value for the reaction output for each reaction. (where $i = 1,2, 3,…16$)

Alkali Lignin is used as the modeling compound for Lignin, which has an empirical formula of $C_{108}H_{107}O_{37}$ and an average unit molecular

Fig. 3. Reaction pathways of Lignin in hydrothermal conditions.

weight of 1996 g/mol per unit [36]. Additionally, for the modeling procedure, an average molecular weight of 10 kg/mol is used, which is the same value Matsumara et al. [8,9] used. Thus, it is assumed that the lignin structure consists of 5 Alkali lignin units. During the calculations, all the components are normalized to 1 atom 'C' per molecule for the simplification. The term 'TOC' is used to indicate the soluble organics in the aqueous phase from lignin hydrolysis except for Lignin, Aromatic hydrocarbons (includes naphthalene, benzene, toluene), catechol, guaiacol, and phenol. In the results section, the term 'biocrude' is used to refer to the cumulative value of Aromatic hydrocarbons, catechol, guaiacol, and phenol. Here Lignin is considered as the biomass. Therefore, it does not belong to TOC, although it is soluble in water. Biocrude is assumed to consist of aromatic hydrocarbons, catechol, guaiacol, benzene, toluene, and phenol. Although benzene and toluene are slightly soluble in water, in this model, they are a part of the biocrude phase. Thus, those chemicals are not included in TOC.

2.4. Hemicellulose hydrolysis model

Hemicellulose hydrolysis model is based on the work from Pronyk and Mazza and Pinkowska et al. [13,25]. Pronyk and Mazza proposed a monophasic and a biphasic mechanism for hemicellulose hydrolysis, where the monophasic mechanism is chosen to develop this model. Hemicellulose is hydrolyzed into the intermittent product of Xylo-oligomers and then again to xylose. As shown in Fig. 4 below, the hydrolysis products further decompose into derivatives, mainly furfural. In this model, furfural is used as the final derivative from the liquefaction, due to the lack of availability of kinetic data. For the hemicellulose hydrolysis model, required kinetic parameters are taken from the literature [13,24–26,26].

Table 3 shows the reaction type of each reaction used in the hemicellulose liquefaction model.

Eqs. (35) and (36) show the reactions incorporated in the hemicellulose liquefaction model.

$$Hemicellulose + e_1 H_2O \xrightarrow{k_{27}} f_1 xylose \tag{35}$$

$$xylose \xrightarrow{k_{28}} f_2 (Biocrude) \tag{36}$$

e_i is the stoichiometry value for water for each hydrolysis reaction. (where $i = 1$)

f_i is the stoichiometry value for the reaction output for each reaction. (where $i = 1,2$)

'*Biocrude*'' is supposed to be a mix of chemicals such as furfural and aldehydes. Literature available on hemicellulose hydrolysis contradicts each other occasionally. According to Pronyk and Mazza [13], conversion of xylose into furfural is about 4% from potentially available xylose in the system. Moreover, the hemicellulose hydrolysis starts around 403 K, and the Xylo-oligomers and monomers available in the system maximize around 443 K [13]. The maximum furfural percentage recorded during the experiments is around 443 K, which is still beyond the temperature range considered in this model. Meanwhile, the pentose sugar arabinose present in hemicellulose could make the hydrolysis more susceptible to the lower temperatures [13]. In the Meantime, according to Pinkowska et al. [25], the maximum yield of saccharides such as xylose is obtained around 508 K. Then the increasing temperatures favored the conversion of saccharides into furfurals, aldehydes, and carboxylic acids. Möller and Schröder [26] observed a maximum furfural yield of 49% at 473 K from xylose conversion, while xylan conversion provides a maximum of around 13% of furfural.
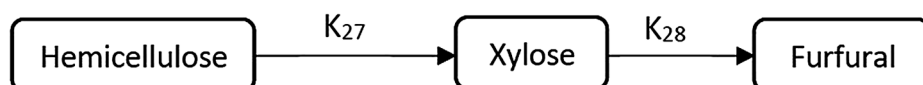
Table 3
Reaction type of each reaction used in hemicellulose liquefaction model.

Reaction	Reaction type	Reaction	Reaction type
K_{27}	Hydrolysis	K_{28}	Dehydration

Moreover, following the results from Pinkowska et al. [25] and Pronyk and Mazza [13], the requirement of lower temperatures (433 K-453 K) for the xylan hydrolysis on producing xylose is observed. From all these studies, it is evident that the hemicellulose hydrolysis occurs and gives the best furfural yields at low temperatures from 403 K to 493 K. During this study, lack of kinetic data, as well as the less contribution of hemicellulose degradation products to the wood hydrolysis process, are observed. Nevertheless, a simple two-stage hemicellulose hydrolysis model is developed base on the available literature. Due to the lack of kinetic data availability on char production of hemicellulose hydrolysis, char is not considered as a degradation product from hemicellulose. Although the temperatures required for better furfural yields from hemicellulose hydrolysis is not within the temperature range considered in this model, still the hemicellulose hydrolysis data is included in the model to perform the wood hydrolysis.

2.5. General assumptions and simplifications

The wood particle is considered as a spherical particle with a given radius in this model. It is submerged in an infinitely large water volume, much larger than the radius of the particle. Hence the dilution of the hydrolysis products is assumed to be infinite at a given distance from the particle center. In this model, it is assumed that there is always enough water in the system to perform all the required hydrolysis reactions. The particle decomposition is assumed only in the radial direction. Therefore, during hydrolysis, the particle is decomposed in the radial direction. Thermophysical properties are presumed to be constant throughout the process as well. The temperature of the particle is always supposed to be equals to the temperature of the fluid surrounding it. As the particle is assumed to be homogenous in properties and composition, no mass transfer is considered, and no accumulation of products from the hydrolysis in the particle is considered. Furthermore, the primary char and secondary char from the reactions are considered as one.

It is learned that an ash layer and an oily film is developed around the shrinking core during the hydrolysis process [7]. Therefore, in the next phase of this model, the effect and behavior of such an ash layer and an oil film are studied and developed. Thus, in this model, it is assumed that all the products from hydrolysis leave the particle surface and does not form a layer on the outside of the wood particle. Hence, water monomers can proceed to the particle and continue the hydrolysis reaction. Besides, wood hydrolysis is modeled as the cumulative effect of the hydrolysis of the three main components of wood. Therefore, the hydrolysis of each model component is modeled separately. Each model component starts hydrolysis at different temperatures and emits hydrolysis products to the system. When each model component hydrolyzes, the radius is assumed to be reduced in a rate that correspondent to the rate constant of hydrolysis of the specific model component.

As described in the assumption section, hydrolysis of Cellulose, Lignin, and Hemicellulose occurs only on the surface of the particle at a given time. In the model, char is produced in two different ways. For the simplification, char produced by dehydration is considered as a direct degradation product of cellulose and lignin hydrolysis.
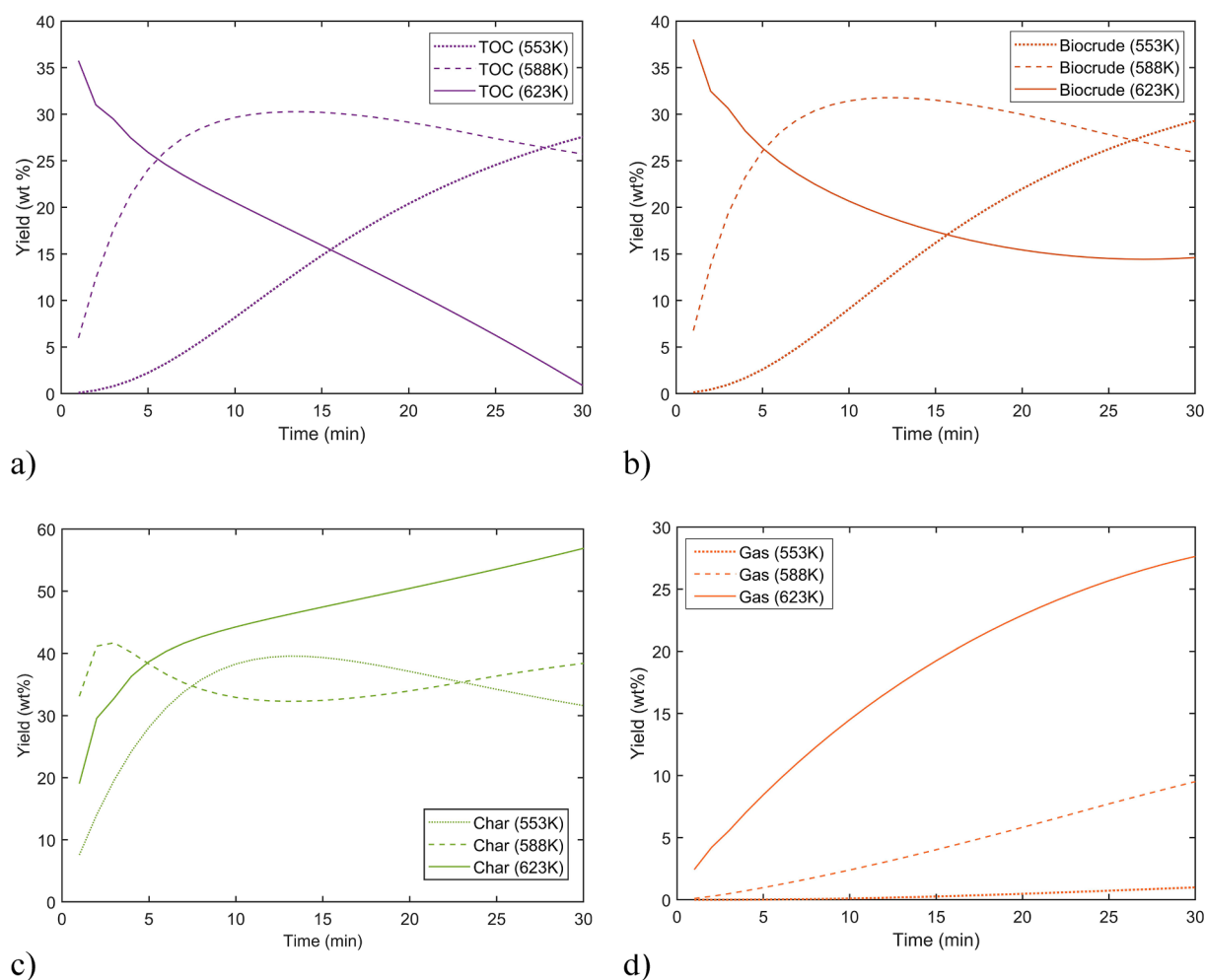

Fig. 4. Reaction pathways of hemicellulose in hydrothermal conditions.

Fig. 5. Effect of temperature on hydrolysis of Cellulose derived outputs at 553 K, 588 K, and 623 K a) TOC b) Biocrude c) Char d) Gas.

Dehydration happens throughout the particle volume, and this leads to the particle becoming more charred with time. When the Carbon content of the particle is increased, it enforces a restriction on the capability of water to react with the wood components. Therefore, unreacted highly charred biomass could have remained in the system. The term primary char stands for this kind of highly charred unreacted biomass. Secondary char (or coke) represents the char produced through the further decomposition of the biocrude and aqueous phase [3,7]. Although char consists of these two components, the presence of secondary char in the resultant of the liquefaction process is small [7]. It is assumed that ash does not participate in reactions.

The composition of the particle is not changed with time or with the hydrolysis reaction. The particle is decomposed only in the radial direction, and the decomposition is dependent only on the biomass left in the particle and the concentration of water in the system. As the reactions proceed, the hydrolysis products are dissolved in the water, and the further hydrolysis reactions of the particle are not affected by the diluted products.

A simplified elemental balance is used for the model by using an approximation for oxygen and hydrogen balance in each compound. Therefore, only Carbon balance is given importance in the modeling process due to the simplification of the calculations. According to Yong and Matsumara [9], H_2 and CO_2 are present in the gas phase in lignin hydrolysis, with CO_2 being the major contributor. Nevertheless, the CO_2

percentage increased with increasing temperature in the subcritical region, and H_2 is decreased with time. Therefore, for the gas phase, CO_2 is used as the model compounds since CO_2 is the principal component in the gas phase.

The stoichiometry for the hydrolysis reactions is calculated based on the experimental results available in the literature. To define the stoichiometry as many as three experimental data are considered in most of the reactions. However, due to the lack of literature, the stoichiometry for some reactions are determined based on a single experimental work. To determine the stoichiometry for each reaction, a set of stoichiometric coefficients for each reaction is calculated, which has a minimum of residual sum of squares (i.e., the difference between the calculated and available experimental values). Mosteiro-Romero et al. [3] showed the product distribution in each holding temperature is the same at all temperatures from 523 K – 623 K. Thus, it is assumed that the determined stoichiometry is the same at each holding temperature and valid throughout the temperature range, which the model is using. Then, at the considered temperature values, the experimental data is fit to the equations. As the experimental data for water is not available, different stoichiometric values for the hydrolysis reactions are calculated using hydrogen and oxygen balance.

Furthermore, due to the lack of literature, especially on the heating stage and of fast reaction kinetics, some of the kinetic data is modified and fit to reactions equations to obtain the yield values in the literature.
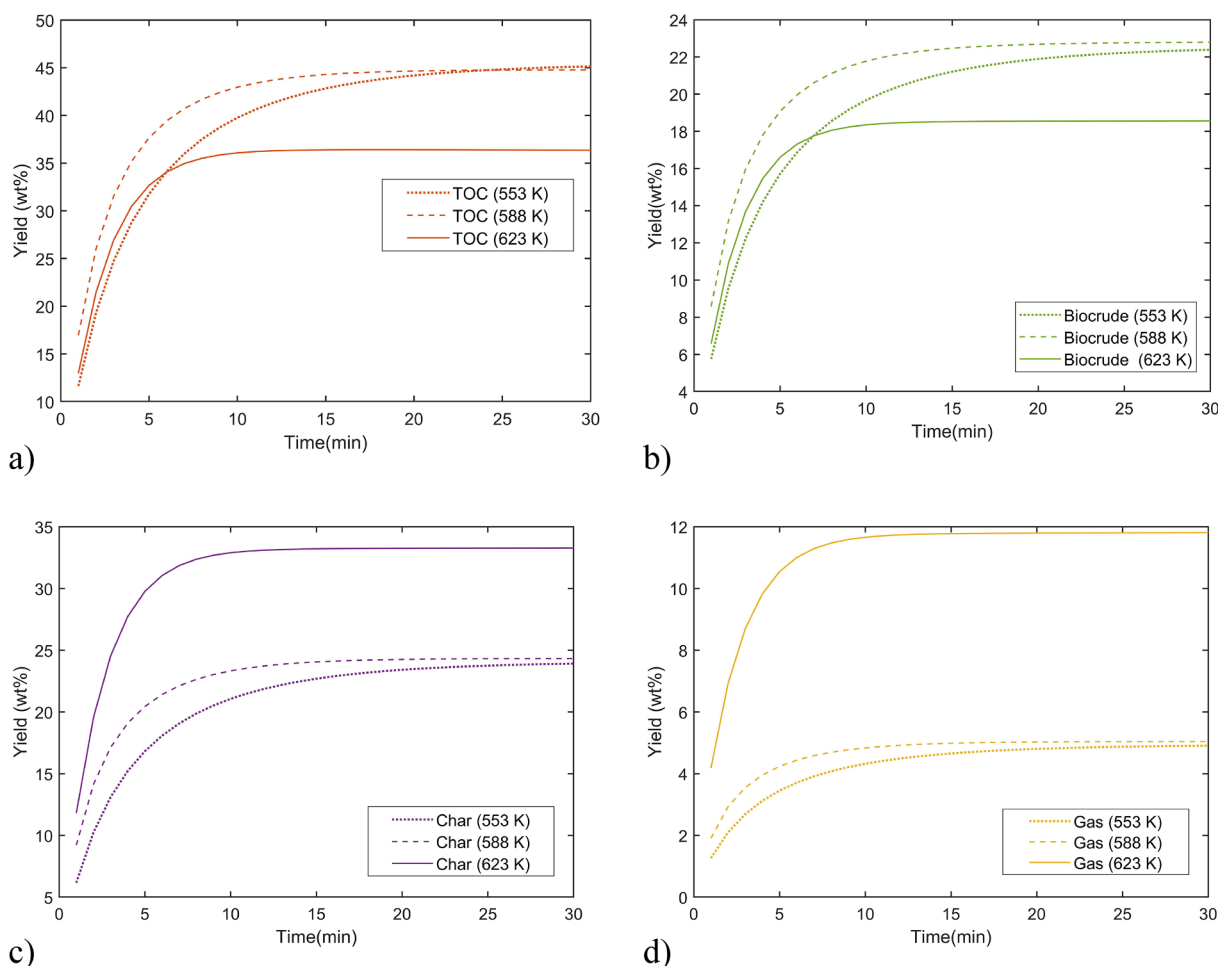
Fig. 6. Effect of temperature on hydrolysis of lignin-derived outputs at 553 K, 588 K, and 623 K a) TOC b) Biocrude c) Char d) Gas.

It could be a possible reason for some of the over predictions and under predictions in the model. The differential equations developed in the mathematical model are solved and discretized in MATLAB R2019b.

3. Results and discussion

3.1. Model predictions

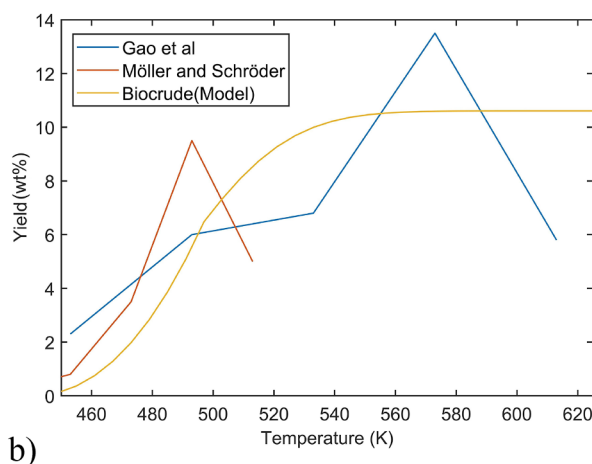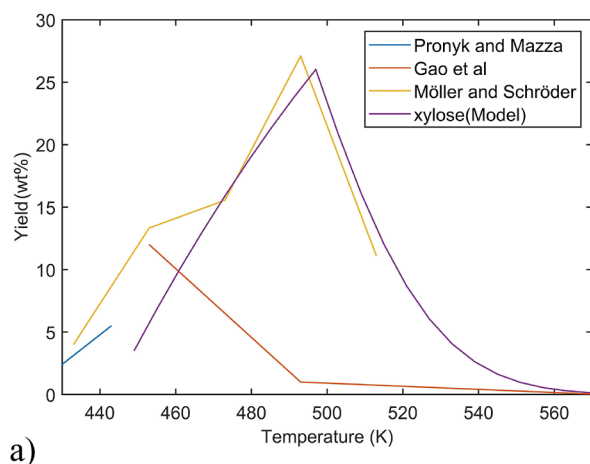In this section, different predictions from the developed model are

illustrated. First, the impact of temperature increase on each wood component hydrolysis and wood hydrolysis is discussed. Subsequently, the impact of residence time, the impact of heating rate on product yield, and the effect of biomass particle size are also explained.

3.1.1. Effect of temperature on the product composition

Fig. 5 shows the impact of temperature variation on cellulose hydrolysis, where Fig. 5a, 5b,5c, and 5d show the variation of TOC, biocrude, char, and gas yield, respectively. Three temperature values

Fig. 7. Effect of temperature on hydrolysis of hemicellulose-derived outputs a) xylose b) biocrude.

(553 K, 588 K, and 623 K) are used to observe the effect of temperature on the yields. According to Fig. 5, char and gas yields become much higher with the increase of temperatures while biocrude and TOC levels go down.

In this model, both primary and secondary char is considered. Therefore, with longer resident times and higher temperatures, higher char yields can be justified. These high yields can be possible, mainly due to the increase of char in secondary reactions. Subsequently, water-soluble organics and light aldehydes in the aqueous phase (TOC) could convert into char and biocrude (5-HMF and furfural, etc.) with further homogeneous hydrolysis reactions and secondary char reactions. Similar variations are observed in work done by Kamio et al. [10,11] Minowa et al. [19], Cantero et al. [21], and Sasaki et al. [14,15,17], where the gas and char yields become notably close to the supercritical region. According to Minowa et al. [19] char can be a decomposition product of further hydrolysis of soluble methanol products, which helps the observations above.

Char was not considered as an output product of the hydrolysis model by Kamio et al. [10,11]. Consequently, they managed to obtain a higher biocrude yield in their model with increasing temperature. It can be mainly due to not having a char phase in their model. As this model has char yields incorporated, the reduction of biocrude yields with higher temperatures can be examined.

Fig. 6 below shows the impact of temperature on lignin-derived product variation. Lignin hydrolyzed quickly into the hydrolysis products due to the rapid kinetics. Fast hydrolysis of Lignin is observed in the available literature [8,9,23,33,37]. Following the cellulose hydrolysis pathway, more char and gas yields are produced by higher

temperatures. Sauer et al. [37] proposed that the desired liquefaction of Lignin is between 553 K and 653 K, which is observed with this model as well.

Fig. 7 below illustrates the behavior of xylose and biocrude created from hemicellulose. Hemicellulose hydrolysis reaction path follows the hydrolysis reaction pathway of Cellulose to some extent. Since only the xylose and biocrude phases are modeled, many observations cannot be made with hemicellulose hydrolysis. Nevertheless, the formation of biocrude can be understood with higher temperatures. Pronyk and Mazza [13] showed that the hydrolysis of hemicellulose could be observed at low temperatures, such as 443 K in minimal percentages.

Furthermore, a shallow conversion of xylose into biocrude at 443 K is illustrated [13]. According to Fig. 7.b), xylose percentage comes to a maximum of around 500 K, which is within the ranges presented by Pronyk and Mazza [13] as well as Pinkowska et al. [25]. With the temperature rise following the conclusions in literature, xylose shows a maximum close to 500 K. At 560 K, the yield of xylose is almost zero. Therefore, the impact of hemicellulose on the cumulative result is almost zero in the temperature range of 553 K to 623 K. Since the temperature range considered in this study is from 553 K to 623 K, the impact of hemicellulose on the cumulative result is not considered.

With the cumulative hydrolysis effect of each wood component, the wood hydrolysis is modeled. Fig. 8 shows the variation of hydrolysis product yields with the increasing temperatures. The term' TOC' is used to represent the aqueous phase in wood liquefaction. Gas and char components are increased expressively at 623 K while the TOC and the biocrude phase decreased significantly. The higher temperatures close to supercritical conditions promote hydrothermal gasification rather
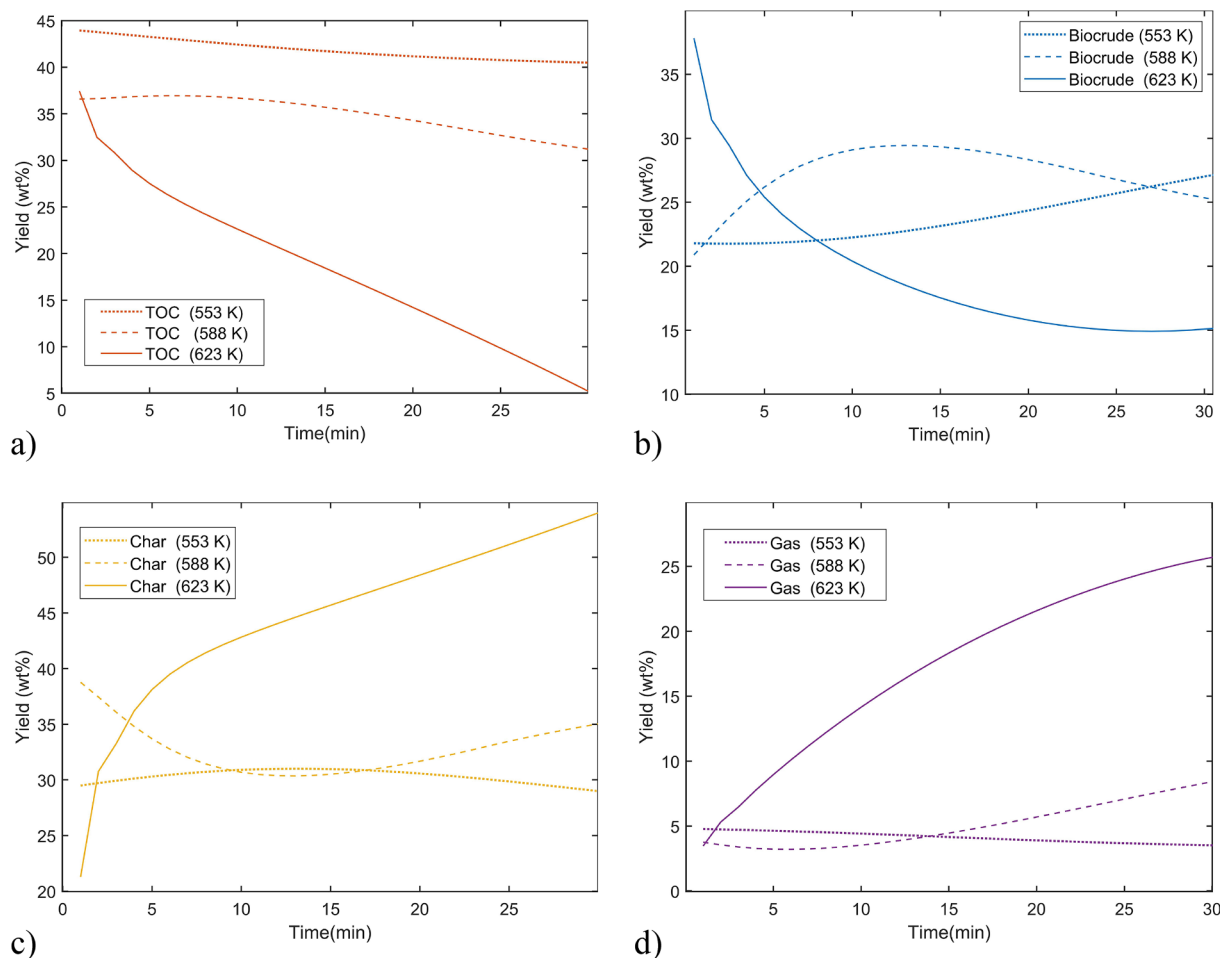

Fig. 8. Effect of temperature on wood as a cumulative effect of hydrolysis of Cellulose, hemicellulose, and lignin-derived outputs at 553 K, 588 K and 623 K a) TOC b) Biocrude c) Char d) Gas.
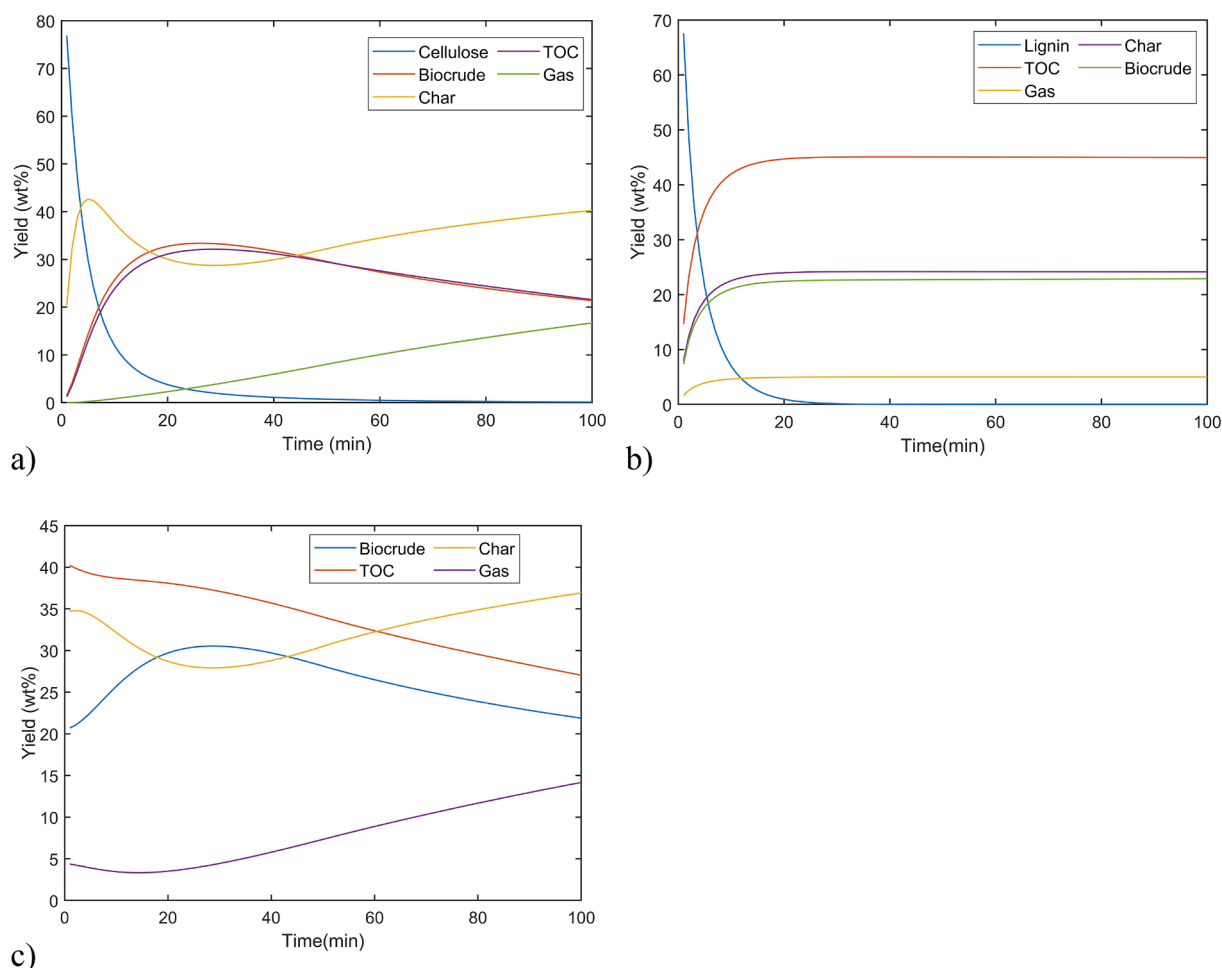
Fig. 9. Effect of residence time on hydrolysis at 573 K a) cellulose b) lignin c) wood.

than liquefaction [38]. That could be the main reason for the dramatic decrease in TOC and the increase of the gas phase. When scrutinized, overall wood hydrolysis product variation slightly follows the cellulose hydrolysis component variation. A significant increase in char yields is observed due to the higher char yields obtained at higher temperatures by cellulose hydrolysis. Shoji et al. [4,5] observed similar variations in wood hydrolysis experiments they performed, where they examined high char yields at higher temperatures. Furthermore, the improvement of biocrude yields, up to some temperature value until it is reduced again, facilitating further reactions to produce more char and gas [3–5,38].

3.1.2. Effect of residence time on the product composition

The residence time of the liquefaction process is one of the crucial parameters of the process. Fig. 9 below shows the variation of products of Cellulose, Lignin, and wood hydrolysis. In this scenario, a residence time of 100 min is used at 573 K.

According to the above Fig. 9a, cellulose hydrolysis shows an increase in char and gas yields with longer residence times. Furthermore, TOC and biocrude yields show an initial rise, followed by a gradual reduction of the yields. Although lignin hydrolysis (Fig. 9b) does not show a significant increase in the yield percentages, the product yields rise to their maximum values much quicker due to the relatively fast decomposition of Lignin. In the end, char yields again are the primary output at longer residence times due to further chain reactions and inter reactions between hydrolysis components.

According to Fig. 9c, wood hydrolysis products are significantly led by the char yields with longer residence times while it shows a decrease

until about 30 min of residence time. Meanwhile, biocrude shows a gradual reduction at longer residence time, which can be observed in Mosteiro-Romero et al. [3,7]. Gas yields follow the behavior of char yields during the whole reaction time, showing an increase in values after 20 mins of residence time. That may be due to the higher conversion of biocrude and TOC into char and gas at longer reaction times. Showing accordance with experimental work from Boocock and Sherman [39], Cellulose and wood hydrolysis show a reduction in biocrude yields with longer residence times with this model.

Many researchers investigated the effect of residence time on product yields [3,40,41]. Boocock and Sherman [39] figured out the longer residence times could reduce the biocrude yields except for the very high loading conditions. Wadrzyk et al. [40] showed the negative effect of higher temperatures and longer residence times on char yields where Yj et al. [42] found out the improvement of liquid yields with longer residence times are negligible. Therefore, the model predictions are following all these observations in literature except the studies by Wadrzyk et al. [40] and Yj et al. [42].

3.1.3. Effect of heating rate

Three different heating rates (2 K/min, 4 K/min, and 6 K/min) are applied in the model to analyze the impact of the heating rate on the product yields. Fig. 10 below shows the yield variation of cellulose-derived products with different heating rates in a temperature range of 560 K to 640 K. High biocrude yields with lower heating rates are observed with cellulose hydrolysis experiments by Kamio et al. [10,11]. In the proposed model, lower heating rates promote biocrude yields up to 610 K (Fig. 10b) in cellulose hydrolysis, which follows the work done
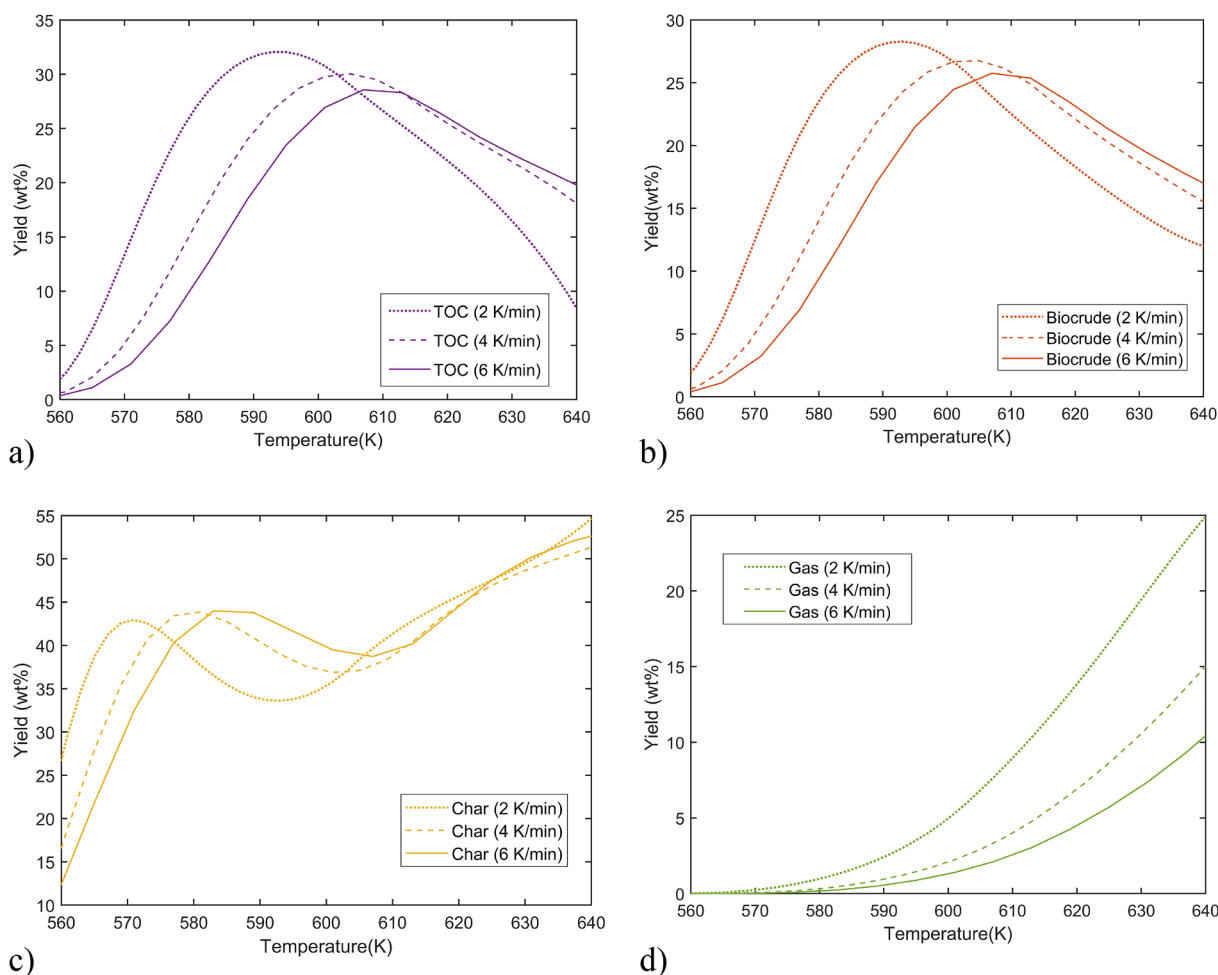
Fig. 10. Effect of heating rate on cellulose hydrolysis) TOC b) biocrude c) char d) gas.
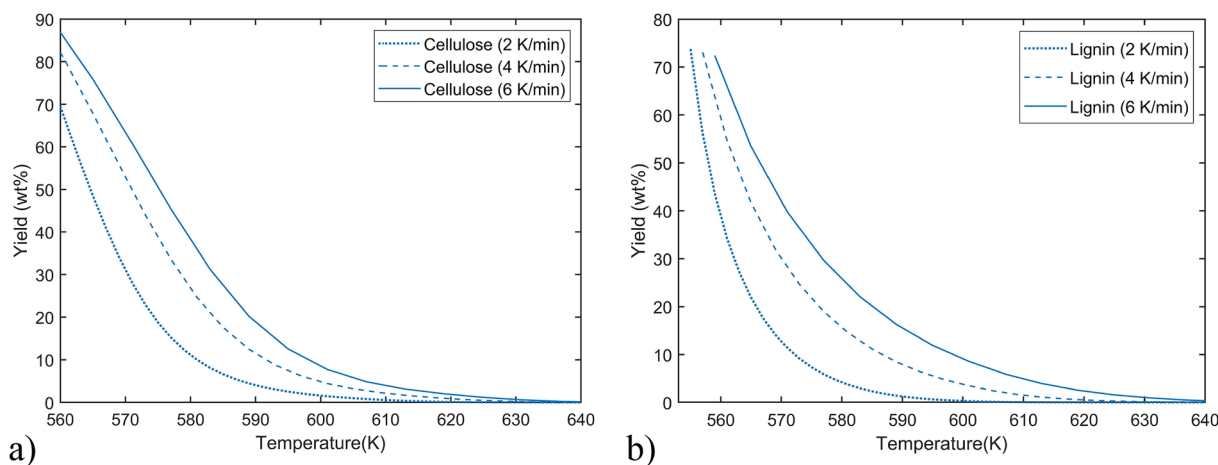

Fig. 11. Effect of heating rate on hydrolysis of a) cellulose b) lignin.

by Kamio et al. [10,11]. Furthermore, Brand et al. [43] obtained a higher biocrude yield with a higher heating rate (20 K/min) for the temperature range 553 K-623 K. The proposed model produced results which are coincided with Brand et al. [43]. Relatively smaller activation energies can be the reason for the high yields with slower heating rates. Meanwhile, with slower heating rates, the particle can be hydrolyzed longer, which ultimately provides longer residence times.

Higher heating rates tend to promote relatively higher char yields for cellulose hydrolysis. According to this observation, with higher heating rates cellulose component of the particle gets more charred. Further, it is observed that the lower heating rates promote better and quicker hydrolysis and, as a result, helps further decomposition and recombination reactions. This trend is supported by the cellulose liquefaction results by Kamio et al. [10], and wood liquefaction results by Mosteiro-Romero et al. [3,7].

Lower heating rates promote better and faster lignin decomposition (Fig. 11), where it produces maximum yields around 620 K. According to Fig. 12, Lignin does not show a significant change in yields with the
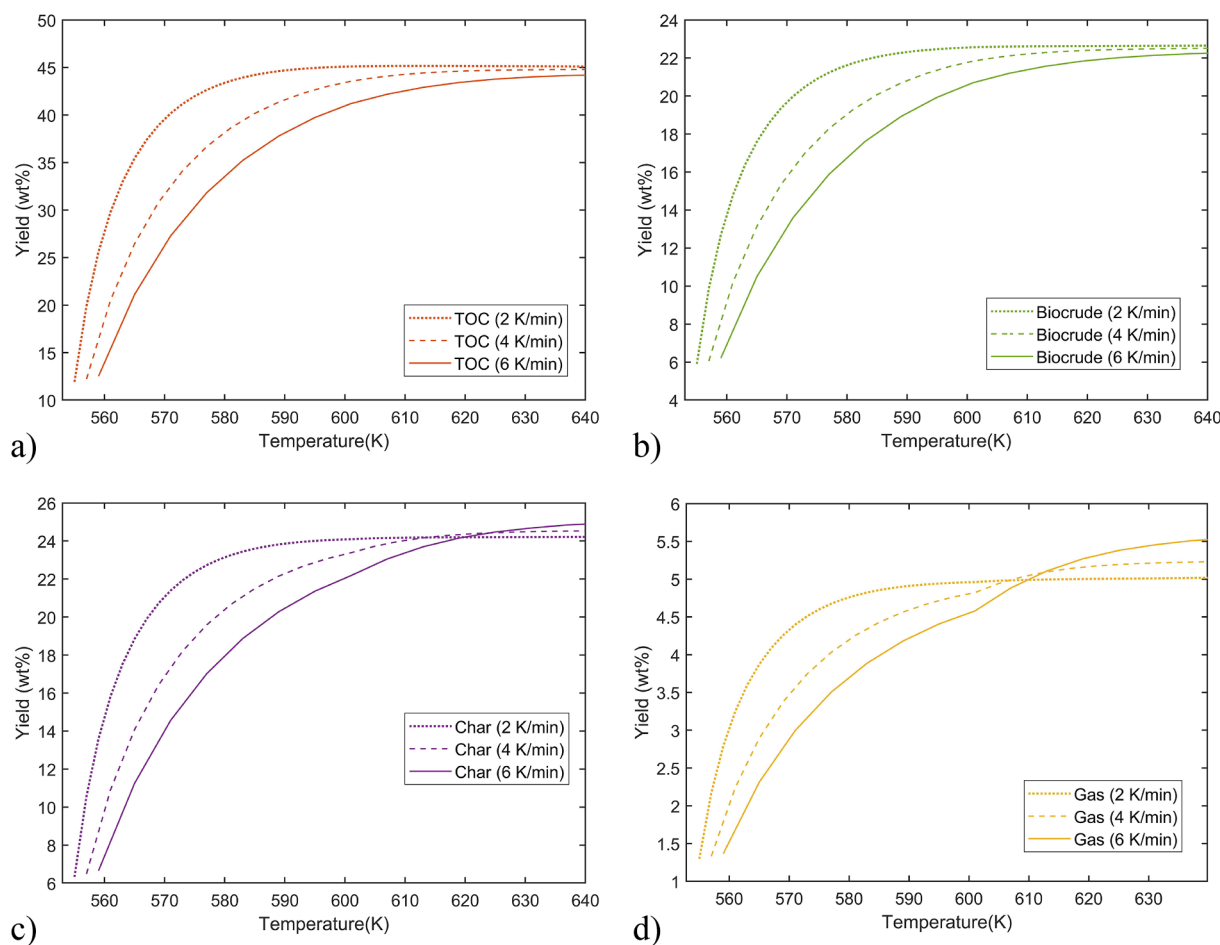
Fig. 12. Effect of heating rate on lignin hydrolysis a) TOC$_L$ b) biocrude c) char d) gas.

heating rate variation. The reason for the slight high yields of outputs in the lower heating rates could be the better decomposition of Cellulose and Lignin in the lower heating rates, as shown in Fig. 11.

Regardless of the heating rate, all the hydrolysis components produced similar percentages of yields with the temperature increase. Besides, char and gas components show an increase in the yield values around 620 K. Slower heating rates have resulted in a faster product yield increase. Ultimately when the temperature value reaches 640 K (the critical point is at 647 K), Product yields have become almost the same value. Therefore, the impact of heating rate is essential only at shorter residence times. Therefore, the heating rate could be a critical aspect of the fast liquefaction concept. In a review study on optimum process conditions for liquefaction, Akhtar et al. [44] showcased the higher heating rates are resulted in higher char yields mainly due to the dominance of secondary reaction. Char yield shows an increase with the higher heating rate close to the supercritical region, justifying that statement by Akhtar et al. [44].

According to the results shown in Fig. 13, for a given temperature value, lower heating rates produce higher biocrude yields until about 600 K, where char yields and gas yields are increased dramatically after 600 K. Initially, higher heating rates produce higher char yields, while after 610 K, higher biocrude and TOC yields are produced. Higher biocrude and gas yields could be due to the lower activation energy of the hydrolysis reactions and longer hydrolysis time. This behavior

coincides with the experimental results from Kamio et al. [10] and Mosteiro-Romero et al. [3,7].

With higher heating rates, initially, the particle gets charred promptly, and it hinders the production of liquid yields initially due to the decreased hydrolysis effect on liquid yields. Nevertheless, at higher temperatures, higher heating rates promote liquid yields than gas and char yields. This increase is, could be due to the higher liquid yields from cellulose liquefaction at higher temperatures with higher heating rates. Besides, 4 K/min and 6 K/min heating rates have imposed a negligible difference on the yields except for the gas component. Therefore, the conclusions made by Akhtar and Amin [44] on the negligible impact of heating rates on wood and each wood component due to the high dissolution and stabilization of decomposed fragments in subcritical water can be justified by the model predictions.

3.1.4. Hydrolysis behavior on particle size

The rationale of the particle size reduction is to provide better accessibility of biomass to the solvent or the liquefaction medium. Nonetheless, as both subcritical and supercritical water are proper heat transfer mediums, change of particle radius makes a low impact on the change of yields [44]. Three sizes of particle radius (0.08 mm, 0.1 mm, and 1 mm) are used as the particle radius. Fig. 14 shows the particle decomposition of Cellulose and Lignin with different particle radius. It is evident with cellulose and lignin hydrolysis graphs as the
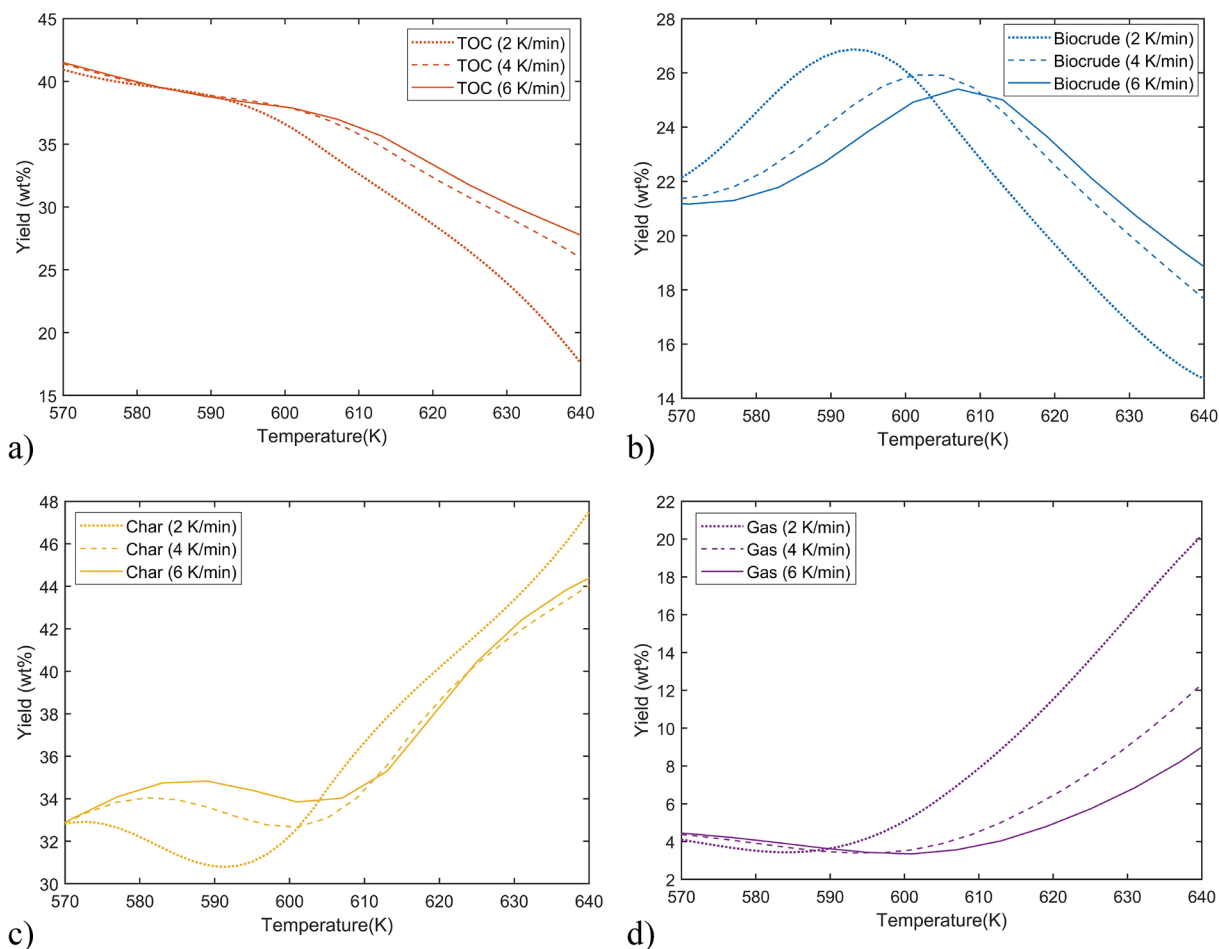
Fig. 13. Effect of heating rate on wood hydrolysis a) TOC b) biocrude c) char d) gas.
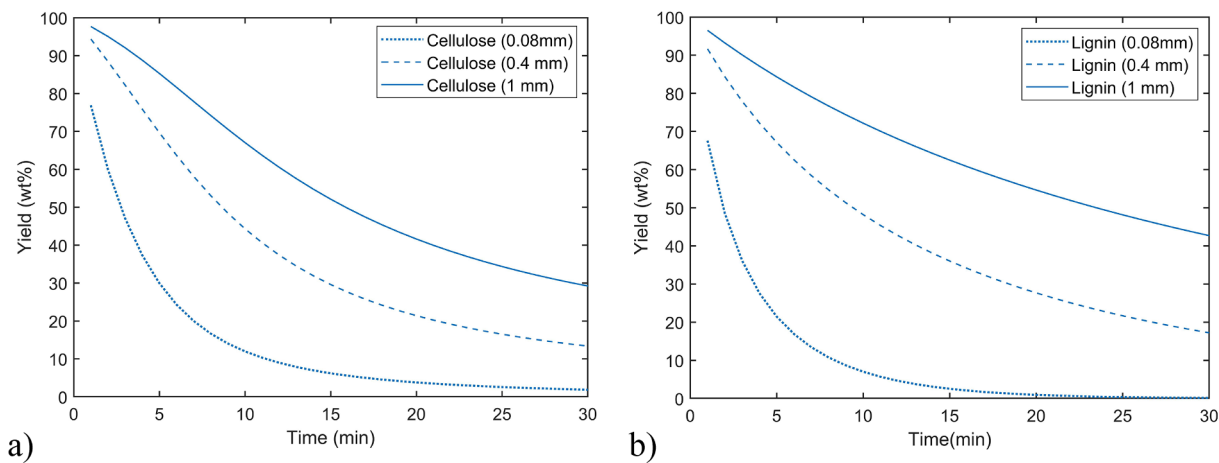

Fig. 14. Effect of particle size on hydrolysis of a) cellulose b) lignin.

decomposition of cellulose and lignin components become much slower with the increase of the radius. Besides, slightly increased char yields are shown with the larger particles. Since the reactions occur on the particle surface, the radius and of the particle could play an essential role in the hydrolysis process.

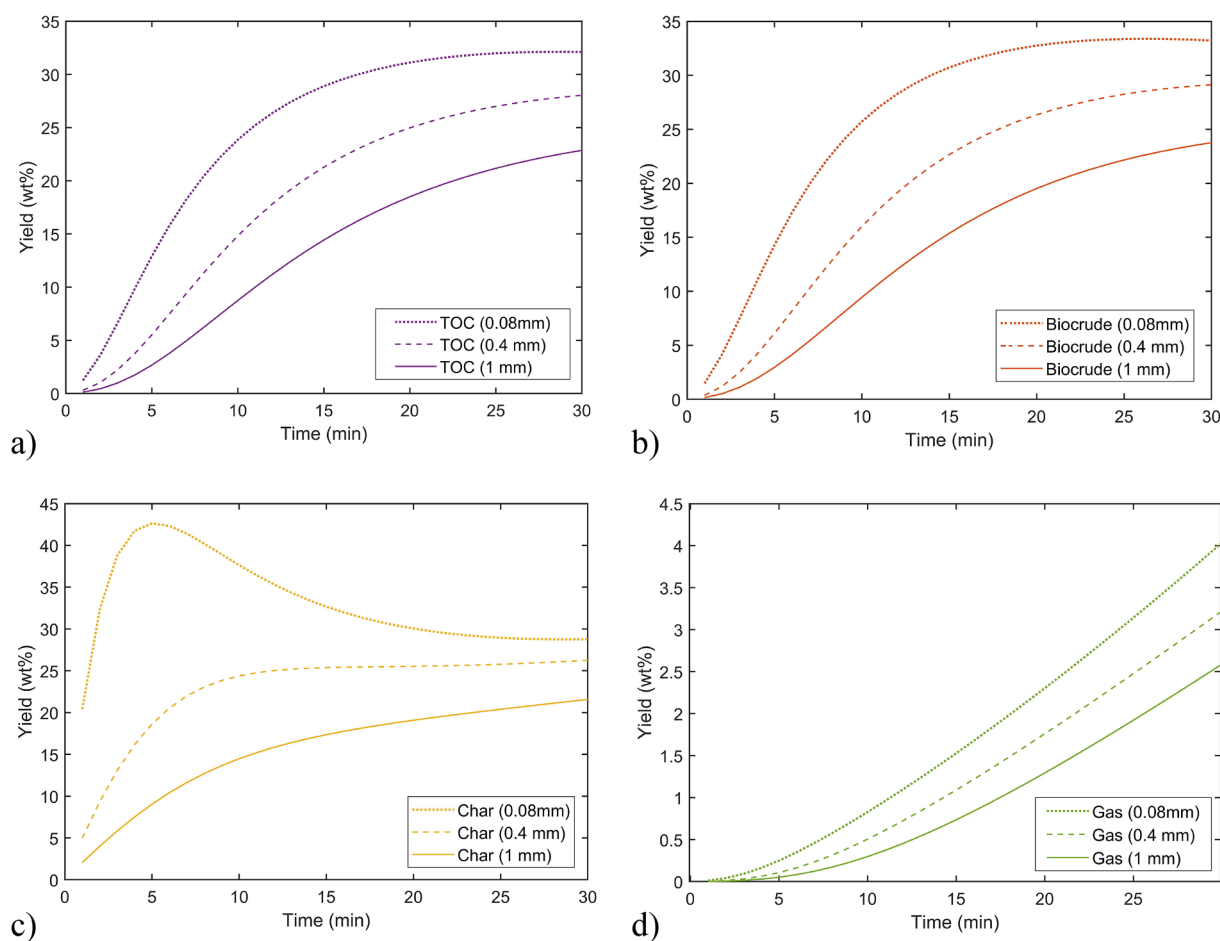Fig. 15 shows the cellulose hydrolysis, and the behavior of Cellulose

Fig. 15. Effect of particle size on hydrolysis of cellulose a) TOC b) biocrude c) char d) gas.

derived components with different particle sizes. The main reason for the smaller particle size to produce more yields is the faster decomposition of the particle. All the particle sizes show the same trend, although the smaller particle size shows a dramatic increase of char yields at the initial stage. This increase could be due to fast kinetics with the smaller particle radius. Besides, the workup procedures could influence the char and bio-oil yields.

According to Fig. 16, Lignin follows the same pattern as Cellulose, where the smaller particle decomposes quickly. Further, faster decomposition has produced higher yields quickly.Fig. 17.

Unreacted biomass is not considered as char, and only the primary and secondary char is considered for the char phase in this model. Therefore, the amount of char produced with larger wood particle size (1 mm) is less. Since the hydrolysis reactions are faster with the smaller particles (0.08 mm), more yield is produced in all the components.

Subsequently, a shrinking core model is employed, the particle radius directly affects the particle decomposition. Moreover, all the reactions have happened on the particle surface. Therefore, for a given temperature and a residence time, yields from the hydrolysis of each wood component, as well as the cumulative model (wood), show

significant changes in the yields. Moreover, the workup procedure affects bio-oil yields as well as char. However, in the literature, experimental work observed that the particle size of feedstock does not play a significant role [45,46]. This statement means the effect of the particle size of the feedstock on the yields is negligible.

3.2. Validation of the model and product composition

Cellulose, hemicellulose, and lignin hydrolysis are considered separately to model wood hydrolysis as the sum of the hydrolysis effect of those three components. To validate each part of the model, each wood component hydrolysis, and hydrolysis of wood is compared with experimental data from the literature in this section.

For the validation of the cellulose hydrolysis model, kinetic data, and process conditions used by Promdej and Matsumara [29] are used for the developed model. Moreover, the model predictions are shown with the experimental data obtained in their study. As shown in Fig. 18, the cellulose hydrolysis model has underpredicted the TOC yields while it has overpredicted the char yield. As the size of the cellulose particles is not provided in the literature, a general radius size of 80 μm is used
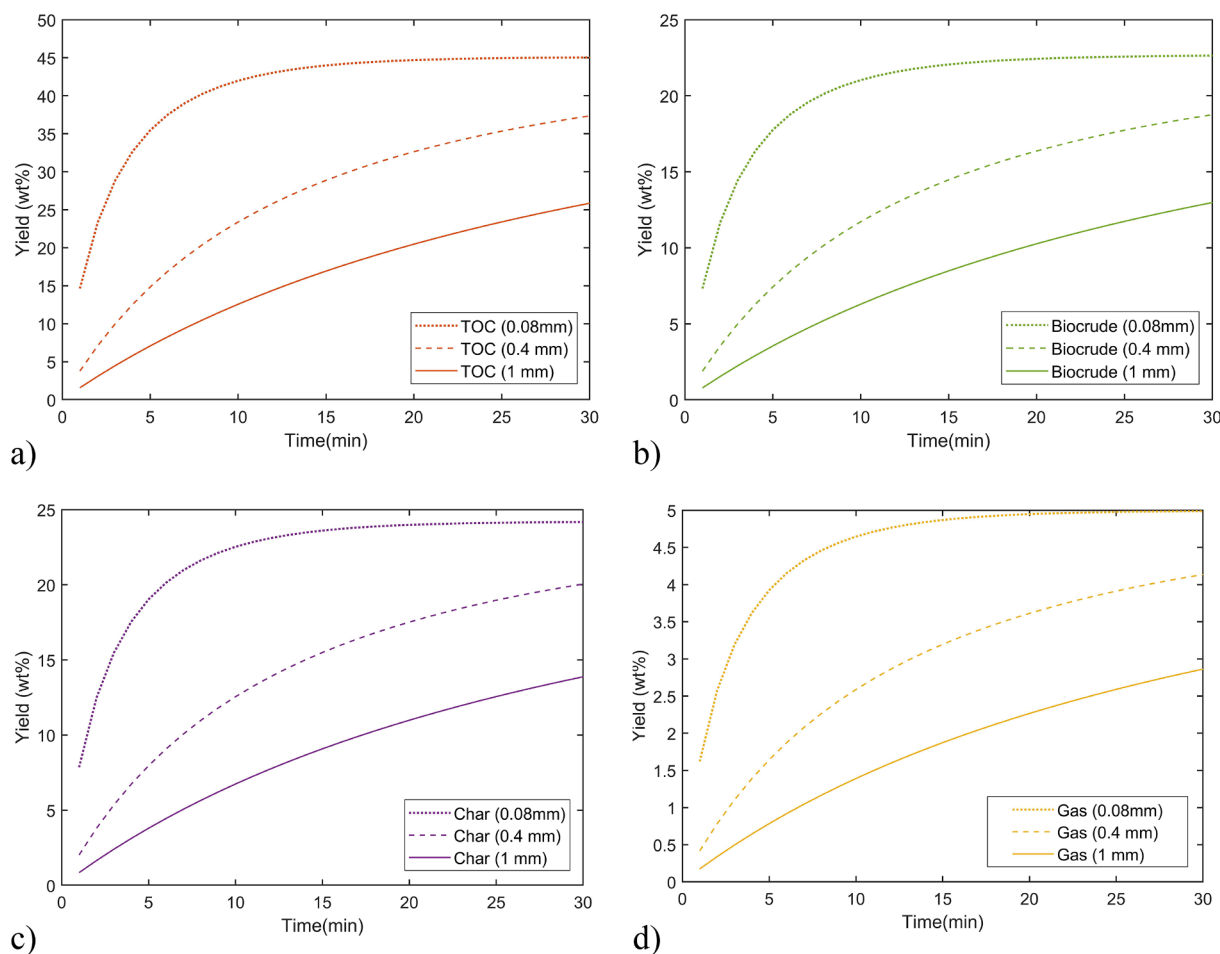
Fig. 16. Effect of particle size on hydrolysis of Lignin a) TOC b) biocrude c) char d) gas.

for the cellulose particle. Furthermore, different loading conditions, different concentrations, and different reaction routes could affect the differences in the yield components. Promdej and Matsumara [29] studied the hydrothermal decomposition of glucose, while in this study, cellulose decomposition is studied. Therefore, kinetic data for cellulose and oligosaccharides hydrolysis are obtained from the literature.

Additionally, kinetic data for cellobiose is used to model the oligosaccharides. For the biocrude phase of the cellulose decomposition, kinetic data for 5-HMF is considered. Besides, biocrude from cellulose consists of many chemicals and compounds. Therefore, these can add another error value for the model predictions too. The same applies to lignin and hemicellulose hydrolysis processes.

To validate the lignin hydrolysis model, experimental work, and kinetic data presented by Yong and Matsumara [9] is used. Below Fig. 19 illustrates the variations of the different phases. In the lignin model, for the simplification, only TOC, gas, char, and biocrude fractions are used for the validation. Like the cellulose validation, different loading conditions, particle sizes, and different process conditions could make impacts on the differences in the considered compounds.

According to Ye et al. [34], increasing temperatures and residence time help promote the decomposition of Lignin and repolymerization of

intermediates to other compounds. Thus, the increase in product yield components with longer residence time can be justified. When the kinetic data from Yong and Matsumara [9] is used, the model predicted yields show a decent fit to the experimental data.

Fig. 20 shows the variation of the xylose and biocrude. Due to the lack of detailed literature, and contradictions in the conclusions in the experimental studies, a simplified hemicellulose hydrolysis reaction pathway is followed, and only the decomposition of hemicellulose to xylose and xylose decomposition to biocrude is modeled. Experimental studies by Pinkowska et al. [25] is used for the development of the hemicellulose hydrolysis model. Experimental results from Pronyk and Mazza [13] Gao et al. [47] and Möller and Schröder [26] are used for the validation of the hemicellulose model. Hemicellulose hydrolysis is noted in temperatures from 403 K to 500 K. With a higher temperature, xylose creation is significantly decreased. Due to this reason, hemicellulose hydrolysis is already finished when the cellulose and lignin hydrolysis is started. Moreover, the hemicellulose hydrolysis temperature range is not considered in this model.

Experimental work from Mosteiro-Romero et al. [3], Sugano et al. [48], Wadrzyk et al. [40], and Qu et al. [41] are used to validate the wood hydrolysis model. The model prediction is based on the
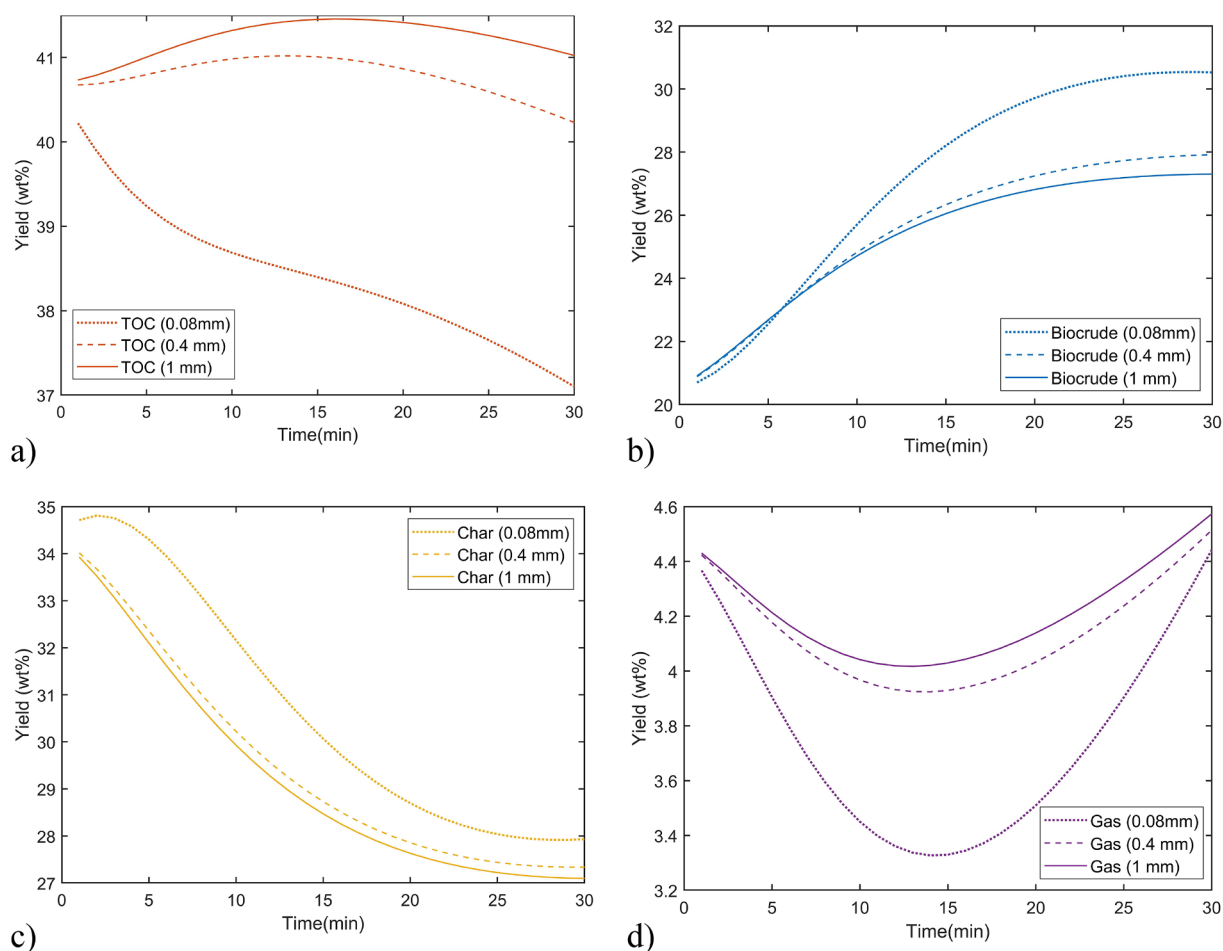
Fig. 17. Effect of particle size on hydrolysis of wood a) TOC b) biocrude c) char d) gas.

cumulative effect of the hydrolysis of three components, while the data from literature are from wood liquefaction. Therefore, thein the validation graphs, the model results, and the actual wood liquefaction data have many differences. For clarity coefficient of determination (R^2) of the model predicted data are calculated and presented with the work done by Sugano et al. [48] since the process conditions and yield calculation method is somewhat similar.

It can be seen that the variation of the wood hydrolysis products follows the path of the cellulose hydrolysis path. Although the biocrude yield prediction can follow the experimental results, char yields are under predicted until 625 K. Besides, in their experimental procedure, the sample is heated for a specific time and then kept at a certain temperature to obtain the outputs. Therefore, at the start of the residence time calculation, there are already some hydrolysis outputs developed. Besides, in the model, it is assumed that the reactor is placed in the heater when the heater comes to a specific temperature. Then as soon as the reactor is started heating, the resident time calculation is started. Thus, initially, the hydrolysis products in the system are zero.

Moreover, in most of the results reported, unreacted biomass is considered as solid residue from the start of the study. Therefore, many studies have shown higher solid residue yield at the start of the residence time. When the biomass is decomposed, unreacted biomass has

reduced, and the char produced is added into the solid residue component. However, in this model, unreacted biomass is not included in the solid residue (char) calculations.

Furthermore, in the experiments, there is some loss of products due to practical difficulties. Then, it can influence the final yields as well. Moreover, in this model, no inter reactions between hydrolysis products from different wood components are considered. As an example, no reactions are considered between cellulose hydrolysis products and lignin hydrolysis products. It can be the next step of this modeling work.

In the model, cellulose lignin and hemicellulose, percentages are predetermined, and for the validation, those predetermined values are used. However, different wood types have different percentages of Cellulose, Lignin, and hemicellulose [6,49]. It can be the main reason for the difference between the liquefaction results in Fig. 21 with experimental results.

4. Conclusion

In this study, wood hydrolysis is modeled for the subcritical region from 553 K to 640 K, utilizing Cellulose, Lignin, and hemicellulose hydrolysis using a shrinking core concept. A kinetic model is fitted with
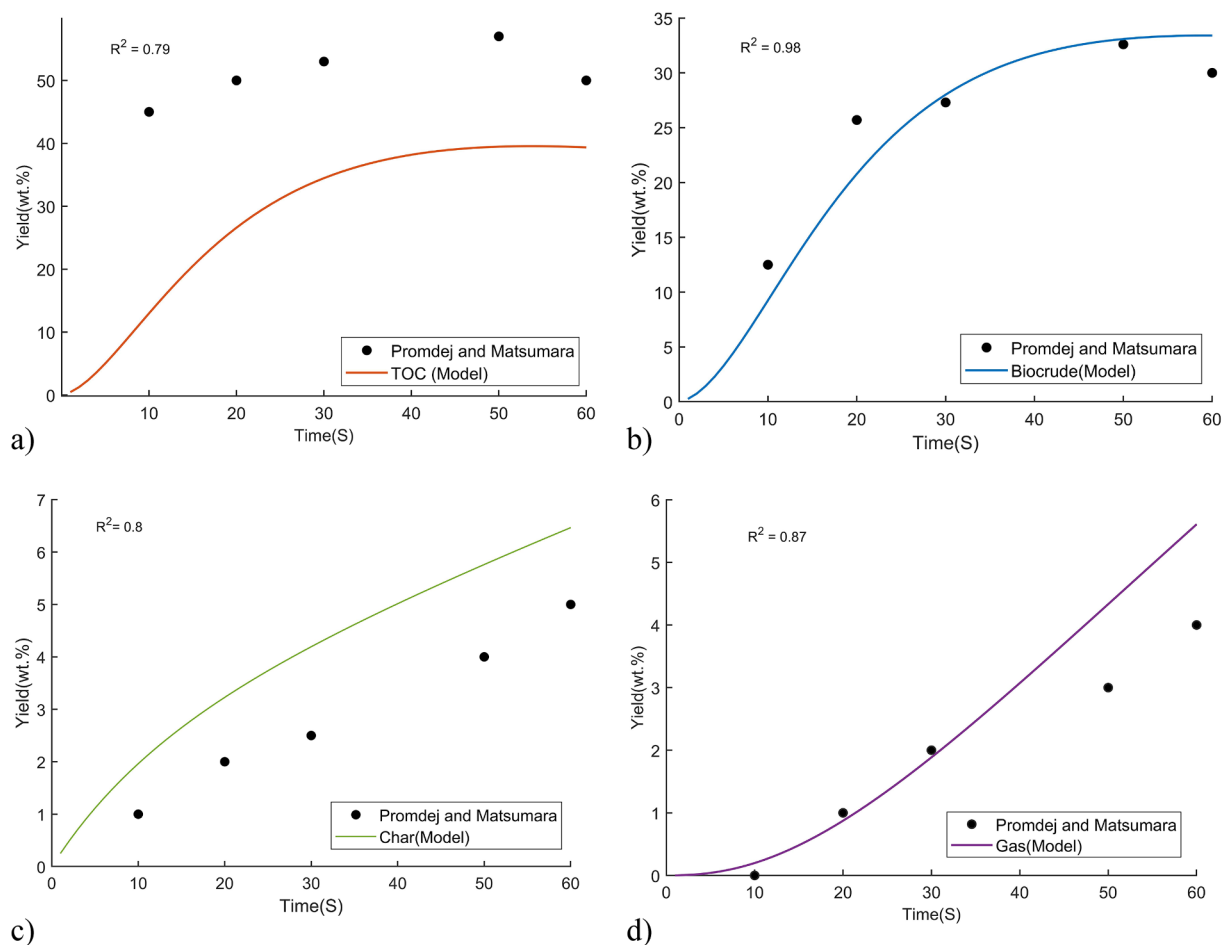
Fig. 18. Cellulose hydrolysis model validation using the kinetic data proposed by Promdej and Matsumara [29] at 573 K. a) TOC b) biocrude c) char d) gas.

the shrinking core model to fit the homogenous reactions in the system. Wood hydrolysis is modeled using the cumulative hydrolysis effect of each wood component.

Hemicellulose hydrolysis occurs around 403 K to 500 K, and the conversion of hemicellulose into xylose becomes negligible in 553 K-640 K. Therefore, for further investigations, Hemicellulose hydrolysis is not considered. The model is validated using cellulose, hemicellulose lignin, and wood liquefaction experimental and model results in the literature. In most of the scenarios, the model shows a reasonable agreement with the available literature. Moreover, the predictions of the model coincide with the literature confirming the reliability of the model. Nevertheless, this model can be developed into a robust model with more inter reactions among the chemicals present in the reaction regime as well to the supercritical region.

At 593 K for a 2 K/min heating rate and particle size of 0.08 mm, biocrude shows the maximum yield of 26.87% for wood liquefaction. Cellulose and Lignin show maximum char and gas yields at 623 K for the same residence time where biocrude and TOC yields show maximum yields at 588 K. Lower heating rates initially promote lignin hydrolysis. Thus, for longer residence times, and close to the critical point, the heating rate does not show a visible impact on the lignin hydrolysis, where char and gas yields of cellulose model show a significant increase. Cellulose hydrolysis shows a big impact on the overall wood liquefaction behavior. Char yields of the cellulose hydrolysis are not affected significantly by the heating rates. After 600 K, wood liquefaction shows higher char and gas yields of 47% and 20%, respectively, with lower heating rates. For maximum operating temperatures, over 600 K TOC and biocrude yields tend to increase the yields. The diameter of the biomass particle has shown a definite impact on the hydrolysis rate of both Cellulose and Lignin.

A limited number of reactions and chemical compounds are used in the model. Furthermore, kinetic data used in the model are found in the literature from various studies under various process conditions. The experimental studies used for validation are operated with various process conditions as well as different workup methods. Therefore, in the validation plots, the model predictions for wood are severely underpredicted or over predicted most of the time. Furthermore, one of the main ideas of developing this model is to observe the difference in the cumulative liquefaction effect of main wood components against actual wood liquefaction. Thus, it is evident that there is an enormous gap between wood liquefaction and modeling wood liquefaction as a cumulative effect of the wood component liquefaction. Since the data used for this model is still too few and bears a high uncertainty in the yields due to the different workup processes, these results should not be used to predict things in a quantitative sense.

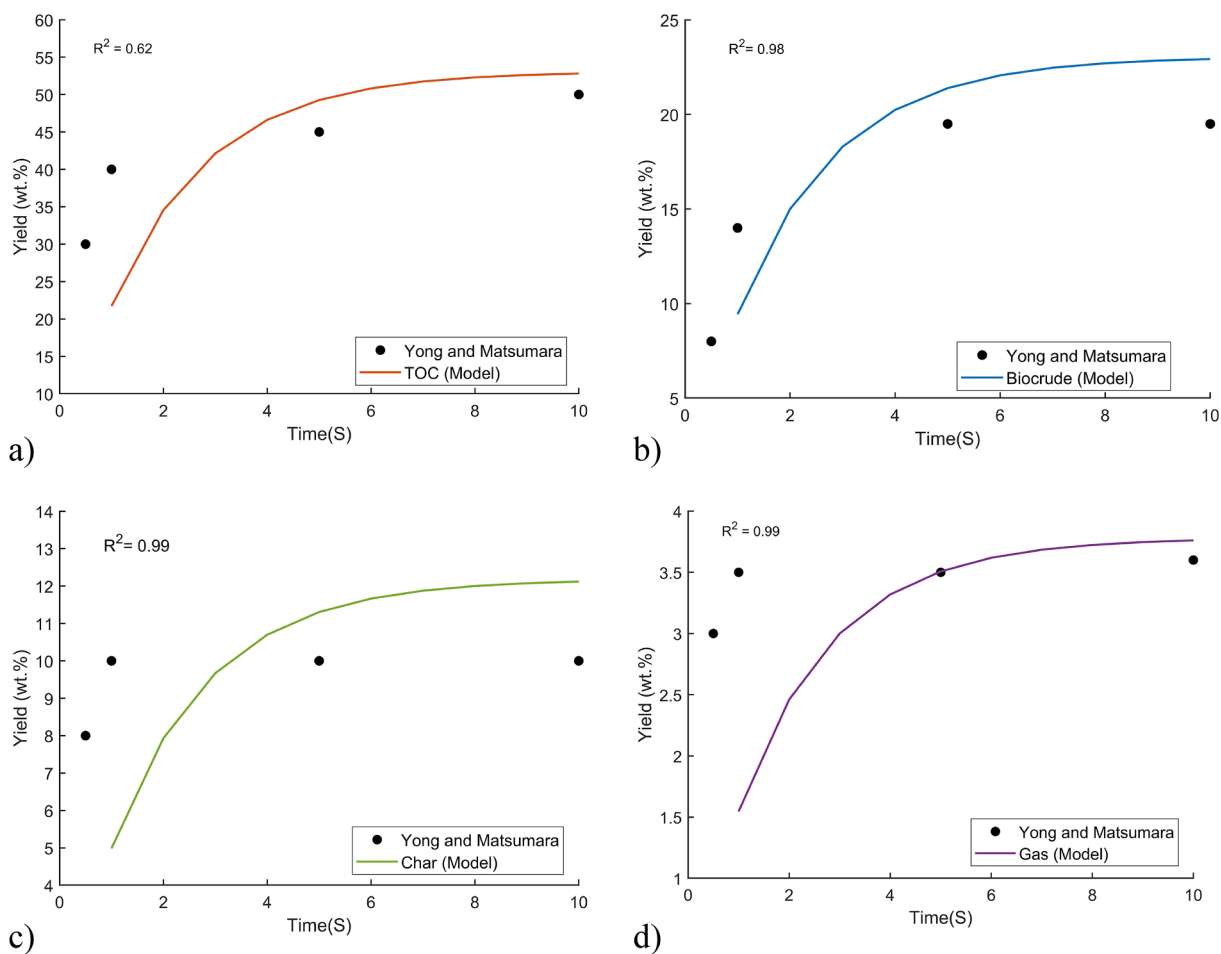**Fig. 19.** Lignin hydrolysis model validation using the kinetic data proposed by Yong and Matsumara [9] at 573 K. a) TOC b) biocrude c) char d) gas.
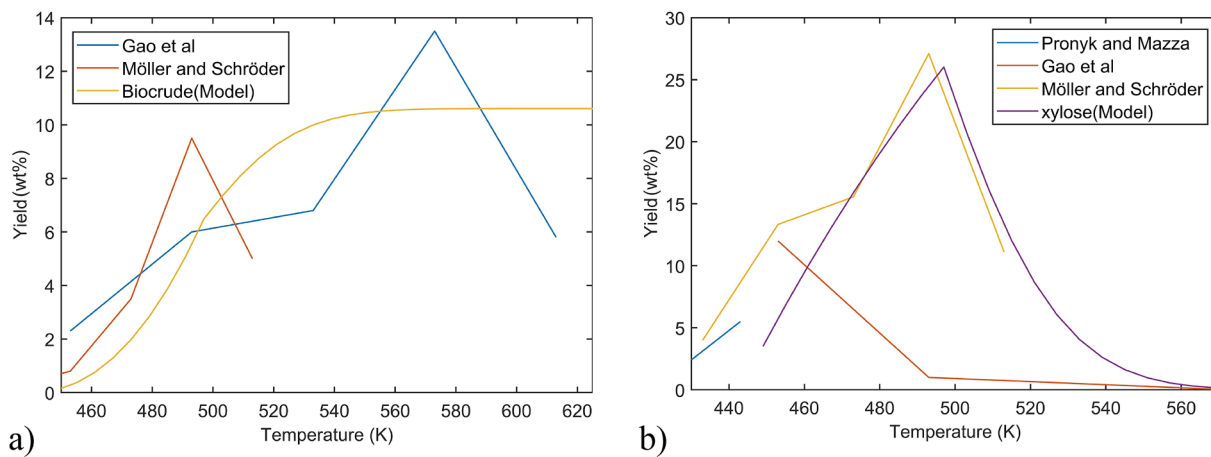

Fig. 20. Hemicellulose hydrolysis validation a) variation of Biocrude b) variation of xylose.
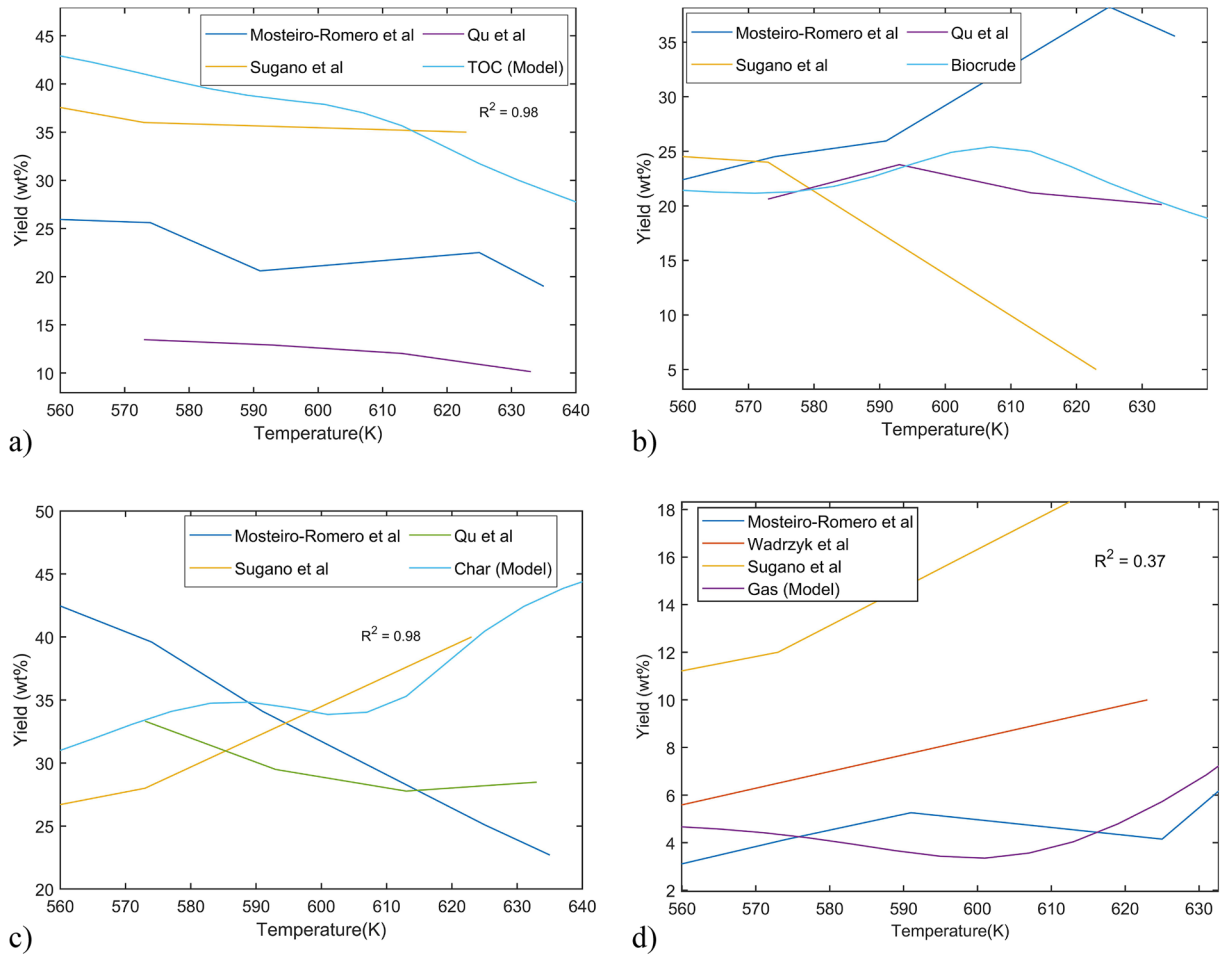
Fig. 21. Wood liquefaction validation with 2 K/min heating rate and a particle size of 80 μm (Coefficient of determination (R^2) is calculated for experimental results from Sugano et al. [48]) a) TOC b) biocrude c) char d) gas.

CRediT authorship contribution statement

Madhawa Jayathilake: Conceptualization, Methodology, Software, Data curation, Visualization, Investigation, Writing - original draft. **Souman Rudra:** Supervision, Writing - review & editing. **Lasse A. Rosendahl:** Supervision, Writing - review & editing.

Declaration of Competing Interest

The authors declare that they have no known competing financial interests or personal relationships that could have appeared to influence the work reported in this paper.

Appendix

Developed differential equations

Cellulose compounds (For 530 K $<$ T)

$$r_{cel} = -k_{x12} C_{cel}^{\frac{2}{3}} \tag{A1}$$

$$r_{oligo,c} = 76.7 k_{x1} C_{cel}^{\frac{2}{3}} - (k_2 + 3k_3) C_{oligo} \tag{A2}$$

$$r_{mono,c} = 3k_2 C_{oligo} - 1.6 k_4 C_{mono} - k_6 C_{TOC,c} \tag{A3}$$

$$r_{MSP,c} = 0.6 k_4 C_{mono} + 0.03 k_3 C_{oligo,c} - 1.9 k_7 C_{toc} - 0.5 k_{10} C_{char} \tag{A4}$$

$$r_{char,c} = 40 k_{x2} C_{cel}^{\frac{2}{3}} + 7 k_{22} C_{TOC,c} + 0.45 k_{10} C_{MSP} \tag{A5}$$

$$r_{TOC,C} = 1.4 k_6 C_{mono} + k_7 C_{MSP} - 0.5 k_8 C_{char,c} - 1.9 k_9 C_{gas,c} \tag{A6}$$

$$r_{gas,C} = 3.3k_9 C_{TOC,c} \tag{A7}$$

Lignin compounds
(For 553 K < T < 603 K)

$$r_{Lig} = -1.5k_{x13} C_L^{\frac{2}{3}} \tag{A8}$$

$$r_{gui,L} = k_{x3} C_L^{\frac{2}{3}} - k_{20} C_{gui,L} - k_{21} C_{gui,L} - k_{22} C_{gui,L} \tag{A9}$$

$$r_{char,L} = 4k_{x4} C_L^{\frac{2}{3}} + 1.5k_{16} C_{Ar} + 2.3k_{17} C_{TOC} + k_{26} C_{Phenol} \tag{A10}$$

$$r_{TOC,L} = 2.5k_{x5} C_L^{\frac{2}{3}} + 0.025k_{21} C_{gui} + k_{24} C_{cat} - (2k_{17} + 2k_{18} + 15k_{19}) C_{TOC,L} + k_{25} C_{Phenol} \tag{A11}$$

$$r_{gas,L} = 4.5k_{x6} C_{gas,L} + 14k_{19} C_{TOC,L} \tag{A12}$$

$$r_{phenol,L} = k_{20} C_{gui,L} + k_{23} C_{cat} - k_{25} C_{Phenol} - k_{26} C_{Phenol} \tag{A13}$$

$$r_{catacol,L} = k_{22} C_{gui,L} - k_{23} C_{cat} - k_{24} C_{cat} \tag{A14}$$

$$r_{Aromatics,L} = 2.6k_{x8} C_L^{\frac{2}{3}} + k_{18} C_{TOC,L} - 2k_{16} C_{Aro} \tag{A15}$$

Hemicellulose compounds (For 433 K < T < 500 K; For T > 500 K, $k_{x14} \ll \lll 1$)

$$r_{hemi} = -0.02k_{x14} C_h^{\frac{2}{3}} \tag{A16}$$

$$r_{xylose,h} = 0.25k_{x14} C_h^{\frac{2}{3}} - k_{27} C_{MSP,h} \tag{A17}$$

$$r_{MSP,h} = 2.5k_{28} C_{xylose} \tag{A18}$$

K_{xi} = Hydrolysis rate constants developed for each hydrolysis reaction using the shrinking core concept
C_{cel} = Concentration of Cellulose in the system
C_{oligo} = concentration of oligosaccharides in the system
C_{mono} = concentration of monosaccharides in the system
$C_{TOC,c}$ = Concentration of TOC produced from cellulose hydrolysis in the system
C_{MSP} = concentration of biocrude products from cellulose hydrolysis of the system
$C_{char,c}$ = concentration of char produced from cellulose hydrolysis of the system
$C_{gas,c}$ = concentration of gas produced from cellulose hydrolysis of the system
C_L = Concentration of Lignin in the system
$C_{gui,L}$ = concentration of guaiacol in the system
C_{Ar} = concentration of aromatic hydrocarbons in the system
$C_{TOC,L}$ = Concentration of TOC produced from lignin hydrolysis in the system
C_{Phenol} = concentration of phenol in the system
$C_{gas,L}$ = concentration of gas produced from lignin hydrolysis of the system

Table A.1
List of kinetic parameters from the literature used as starting points for the frequency factors for each reaction in the computational model.

Kinetic parameter	Value	Kinetic parameter	Value
$K_{0,1}$	7.3×10^6 [a]	$K_{0,15}$	2.15×10^3 [e]
$K_{0,2}$	6×10^7 [b]	$K_{0,16}$	1.02×10 [e]
$K_{0,3}$	3×10^{11} [a]	$K_{0,17}$	2.44×10 [e]
$K_{0,4}$	1.33×10^{10} [c]	$K_{0,18}$	4.47×10 [e]
$K_{0,5}$	8×10^7 [c]	$K_{0,19}$	1.69×10 [e]
$K_{0,6}$	5.5×10^9 [d]	$K_{0,20}$	8.76×10^6 [e]
$K_{0,7}$	1.39×10^9 [c]	$K_{0,21}$	5.79×10^2 [e]
$K_{0,8}$	1.00×10^8 [c]	$K_{0,22}$	3.91×10^3 [e]
$K_{0,9}$	2.89×10^8 [c]	$K_{0,23}$	0
$K_{0,10}$	2.06×10^7 [c]	$K_{0,24}$	0
$K_{0,11}$	9.18×10^2 [e]	$K_{0,25}$	0
$K_{0,12}$	1.74×10^3 [e]	$K_{0,26}$	0
$K_{0,13}$	5.45×10^3 [e]	$K_{0,27}$	2.59×10^6 [f]
$K_{0,14}$	3.13×10^2 [e]	$K_{0,28}$	1.35×10^3 [g]

For all the reactions, a unity reaction order is assumed.
a:- calculated by the data extracted from Sasaki et al. [14,15,17] and Kamio et al. [11].
b: - calculated by the data extracted from Kamio et al. [11].
c:- calculated by the data extracted from Promdej and Matsumura [29].
d:- calculated by the data extracted from Cantero et al. [21].
e:- calculated by the data extracted from Yong and Matsumara [9].
f:- calculated by the data extracted from Möller and Schröder [26].
g:- calculated by the data extracted from Mazza and Pronyk [13].

Table A.2
Constant operational conditions used for the calculations.

Constant parameter used	Value	Unit
Density of Cellulose	555	mol/m^3
Density of Lignin	560	mol/m^3
Density of hemicellulose	555	mol/m^3
K_a	0.001	m/s
C_b	7000	mol/m^3
$T_{initial}$	553	K
r_0	0.00008	m
R	8.314	J/ (K mol)

C_{cat} = concentration of catechol in the system

C_{xylose} = concentration of hemicellulose in the system

C_{xylose} = concentration of xylose in the system

$C_{MSP,h}$ = concentration of biocrude products from hemicellulose hydrolysis

Kinetic parameters (Tables A.1 and A.2)

References

[1] Toor S, Rosendahl L, Rudolf A. Hydrothermal liquefaction of biomass: a review of subcritical water technologies. Energy 2011;36:2328–42. https://doi.org/10.1016/j.energy.2011.03.013.

[2] Barnés MC, de Visser MM, van Rossum G, Kersten SRA, Lange J-P. Liquefaction of wood and its model components. J Anal Appl Pyrol 2017;125:136–43. https://doi.org/10.1016/j.jaap.2017.04.008.

[3] Mosteiro-Romero M, Vogel F, Wokaun A. Liquefaction of wood in hot compressed water: Part 1 — Experimental results. Chem Eng Sci 2014;109:111–22. https://doi.org/10.1016/j.ces.2013.12.038.

[4] Shoji D, Kuramochi N, Yui K, Uchida H, Itatani K, Koda S. Visualized kinetic aspects of a wood block in sub- and supercritical water oxidation. Ind Eng Chem Res 2006;45:5885–90. https://doi.org/10.1021/ie0604775.

[5] Shoji D, Sugimoto K, Uchida H, Itatani K, Fujie M, Koda S. Visualized kinetic aspects of decomposition of a wood block in sub- and supercritical water. Ind Eng Chem Res 2005;44:2975–81. https://doi.org/10.1021/ie040263s.

[6] Zhong C, Wei X. A comparative experimental study on the liquefaction of wood. Energy 2004;29:1731–41. https://doi.org/10.1016/j.energy.2004.03.096.

[7] Mosteiro-Romero M, Vogel F, Wokaun A. Liquefaction of wood in hot compressed water Part 2–Modeling of particle dissolution. Chem Eng Sci 2014;109:220–35. https://doi.org/10.1016/j.ces.2013.12.039.

[8] Yong T-L-K, Matsumura Y. Reaction kinetics of the lignin conversion in supercritical water. Ind Eng Chem Res 2012;51:11975–88. https://doi.org/10.1021/ie300921d.

[9] Yong T-L, Matsumura Y. Kinetic analysis of lignin hydrothermal conversion in sub- and supercritical water. Ind Eng Chem Res 2013;52:5626–39. https://doi.org/10.1021/ie400600x.

[10] Kamio E, Takahashi S, Noda H, Fukuhara C, Okamura T. Effect of heating rate on liquefaction of cellulose by hot compressed water. Chem Eng J 2008;137:328–38. https://doi.org/10.1016/j.cej.2007.05.007.

[11] Kamio E, Sato H, Takahashi S, Noda H, Fukuhara C, Okamura T. Liquefaction kinetics of cellulose treated by hot compressed water under variable temperature conditions. J Mater Sci 2008;43:2179–88. https://doi.org/10.1007/s10853-007-2043-6.

[12] Minowa T, Zhen F, Ogi T. Cellulose decomposition in hot-compressed water with alkali or nickel catalyst. J Supercrit Fluids 1998;13:253–9. https://doi.org/10.1016/S0896-8446(98)00059-X.

[13] Pronyk C, Mazza G. Kinetic modeling of hemicellulose hydrolysis from triticale straw in a pressurized low polarity water flow-through reactor. Ind Eng Chem Res 2010;49:6367–75. https://doi.org/10.1021/ie1003625.

[14] Sasaki M, Adschiri T, Arai K. Kinetics of cellulose conversion at 25 MPa in sub- and supercritical water. AIChE J 2004;50:192–202. https://doi.org/10.1002/aic.10018.

[15] Sasaki M, Kabyemela B, Malaluan R, Hirose S, Takeda N, Adschiri T, et al. Cellulose hydrolysis in subcritical and supercritical water. J Supercrit Fluids 1998;13:261–8. https://doi.org/10.1016/S0896-8446(98)00060-6.

[16] Rogalinski T, Liu K, Albrecht T, Brunner G. Hydrolysis kinetics of biopolymers in subcritical water. J Supercrit Fluids 2008;46:335–41. https://doi.org/10.1016/j.supflu.2007.09.037.

[17] Sasaki M, Fang Z, Fukushima Y, Adschiri T, Arai K. Dissolution and hydrolysis of cellulose in subcritical and supercritical water. Ind Eng Chem Res 2000;39:2883–90. https://doi.org/10.1021/ie990690j.

[18] Karagöz S, Bhaskar T, Muto A, Sakata Y. Comparative studies of oil compositions produced from sawdust, rice husk, lignin and cellulose by hydrothermal treatment. Fuel 2005;84:875–84. https://doi.org/10.1016/j.fuel.2005.01.004.

[19] Minowa T, Fang Z, Ogi T, Várhegyi G. Decomposition of cellulose and glucose in hot-compressed water under catalyst-free conditions. J Chem Eng Jpn 1998;31:131–4. https://doi.org/10.1252/jcej.31.131.

[20] Kabyemela BM, Adschiri T, Malaluan RM, Arai K. Kinetics of glucose epimerization and decomposition in subcritical and supercritical water. Ind Eng Chem Res 1997;36:1552–8. https://doi.org/10.1021/ie960250h.

[21] Cantero DA, Bermejo MD, Cocero MJ. Kinetic analysis of cellulose depolymerization reactions in near critical water. J Supercrit Fluids 2013;75:48–57. https://doi.org/10.1016/j.supflu.2012.12.013.

[22] Zhang B, Huang H-J, Ramaswamy S. Reaction kinetics of the hydrothermal treatment of lignin. Appl Biochem Biotechnol 2008;147:119–31. https://doi.org/10.1007/s12010-007-8070-6.

[23] Forchheim D, Hornung U, Kruse A, Sutter T. Kinetic modelling of hydrothermal lignin depolymerisation. Waste Biomass Valorization 2014;5:985–94. https://doi.org/10.1007/s12649-014-9307-6.

[24] Delbecq F, Wang Y, Muralidhara A, El Ouardi K, Marlair G, Len C. Hydrolysis of hemicellulose and derivatives—a review of recent advances in the production of furfural. Front Chem 2018;6. https://doi.org/10.3389/fchem.2018.00146.

[25] Pińkowska H, Wolak P, Złocińska A. Hydrothermal decomposition of xylan as a model substance for plant biomass waste – hydrothermolysis in subcritical water. Biomass Bioenergy 2011;35:3902–12. https://doi.org/10.1016/j.biombioe.2011.06.015.

[26] Möller M, Schröder U. Hydrothermal production of furfural from xylose and xylan as model compounds for hemicelluloses. RSC Adv 2013;3:22253–60. https://doi.org/10.1039/C3RA43108H.

[27] Galgano A, Blasi CD. Modeling wood degradation by the unreacted-core-shrinking approximation. Ind Eng Chem Res 2003;42:2101–11. https://doi.org/10.1021/ie020939o.

[28] Laidler KJ. The development of the Arrhenius equation. J Chem Educ 1984;61:494. https://doi.org/10.1021/ed061p494.

[29] Promdej C, Matsumura Y. Temperature effect on hydrothermal decomposition of glucose in sub- and supercritical water. Ind Eng Chem Res 2011;50:8492–7. https://doi.org/10.1021/ie200298c.

[30] Klingler D, Vogel H. Influence of process parameters on the hydrothermal decomposition and oxidation of glucose in sub- and supercritical water. J Supercrit Fluids 2010;55:259–70. https://doi.org/10.1016/j.supflu.2010.06.004.

[31] Möller M, Harnisch F, Schröder U. Hydrothermal liquefaction of cellulose in subcritical water—the role of crystallinity on the cellulose reactivity. RSC Adv 2013;3:11035–44. https://doi.org/10.1039/C3RA41582A.

[32] Fang Z, Sato T, Smith RL, Inomata H, Arai K, Kozinski JA. Reaction chemistry and phase behavior of lignin in high-temperature and supercritical water. Bioresour Technol 2008;99:3424–30. https://doi.org/10.1016/j.biortech.2007.08.008.

[33] Arturi KR, Strandgaard M, Nielsen RP, Søgaard EG, Maschietti M. Hydrothermal liquefaction of lignin in near-critical water in a new batch reactor: Influence of phenol and temperature. J Supercrit Fluids 2017;123:28–39. https://doi.org/10.1016/j.supflu.2016.12.015.

[34] Ye Y, Zhang Y, Fan J, Chang J. Novel method for production of phenolics by combining lignin depolymerization and extraction in aqueous ethanol. Ind Eng Chem Res 2012;51:103–10. https://doi.org/10.1021/ie202118d.

[35] Pińkowska H, Wolak P, Złocińska A. Hydrothermal decomposition of alkali lignin in sub- and supercritical water. Chem Eng J 2012;187:410–4. https://doi.org/10.1016/j.cej.2012.01.092.

[36] Marshall HB. The structure and properties of alkali lignin; 1934.

[37] Sauer J, Dahmen N, Hornung U, Schuler J, Kruse A. Hydrothermal Liquefaction of Lignin. J Biomater Nanobiotechnol 2017;8:720–6. https://doi.org/10.4236/jbnb.2017.81007.

[38] de Caprariis B, De Filippis P, Petrullo A, Scarsella M. Hydrothermal liquefaction of biomass: Influence of temperature and biomass composition on the bio-oil production. Fuel 2017;208:618–25. https://doi.org/10.1016/j.fuel.2017.07.054.

[39] Boocock DGB, Sherman KM. Further aspects of powdered poplar wood liquefaction by aqueous pyrolysis. Can J Chem Eng 1985;63:627–33. https://doi.org/10.1002/cjce.5450630415.

[40] Wądrzyk M, Berdel M, Janus R, Brilman DWF. Hydrothermal processing of pine wood: effect of process variables on bio-oil quality and yield. E3S Web Conf 2019;108:02004. https://doi.org/10.1051/e3sconf/201910802004.

[41] Qu Y, Wei X, Zhong C. Experimental study on the direct liquefaction of Cunninghamia lanceolata in water. Energy 2003;28:597–606. https://doi.org/10.1016/S0360-5442(02)00178-0.

[42] Yj Y, J X, Tc L, Zw R. Liquefaction of sawdust for liquid fuel. Fuel Process Technol 1999;60:135–43.

[43] Brand S, Hardi F, Kim J, Suh DJ. Effect of heating rate on biomass liquefaction: differences between subcritical water and supercritical ethanol. Energy 2014;68:420–7. https://doi.org/10.1016/j.energy.2014.02.086.

[44] Akhtar J, Amin NAS. A review on process conditions for optimum bio-oil yield in hydrothermal liquefaction of biomass. Renew Sustain Energy Rev 2011;15:1615–24. https://doi.org/10.1016/j.rser.2010.11.054.

[45] Yilgin M, Pehlivan D. Poplar wood–water slurry liquefaction in the presence of formic acid catalyst. Energy Convers Manage 2004;45:2687–96. https://doi.org/10.1016/j.enconman.2003.12.010.

[46] Sintamarean IM, Grigoras IF, Jensen CU, Toor SS, Pedersen TH, Rosendahl LA. Two-stage alkaline hydrothermal liquefaction of wood to biocrude in a continuous bench-scale system. Biomass Convers Biorefinery 2017;7:425–35. https://doi.org/10.1007/s13399-017-0247-9.

[47] Gao Y, Wang H, Guo J, Peng P, Zhai M, She D. Hydrothermal degradation of hemicelluloses from triploid poplar in hot compressed water at 180–340 °C. Polym Degrad Stab 2016;126:179–87. https://doi.org/10.1016/j.polymdegradstab.2016.02.003.

[48] Sugano M, Takagi H, Hirano K, Mashimo K. Hydrothermal liquefaction of plantation biomass with two kinds of wastewater from paper industry. J Mater Sci 2008;43:2476–86. https://doi.org/10.1007/s10853-007-2106-8.

[49] Feng S, Yuan Z, Leitch M, Xu CC. Hydrothermal liquefaction of barks into bio-crude – Effects of species and ash content/composition. Fuel 2014;116:214–20. https://doi.org/10.1016/j.fuel.2013.07.096.